Exploring protein candidates with enhanced cargo loading capabilities into *Saccharomyces cerevisiae* extracellular vesicles

Alexander Christophe Pawelczak

A Thesis
In The Department
of
Biology

Presented in Partial Fulfillment of the Requirements
For the Degree of
Master of Science (Biology) at
Concordia University
Montréal, Quebec, Canada

January 2024

CONCORDIA UNIVERSITY

SCHOOL OF GRADUATE STUDIES

This is to certify that the thesis prepared

By: Alexander Christophe Pawelczak

Entitled: Exploring protein candidates with enhanced cargo loading capabilities into *Saccharomyces cerevisiae* extracellular vesicles

and submitted in partial fulfillment of the requirements for the degree of

Master of Science (Biology)

complies with the regulations of the University and meets the accepted standards with respect to originality and quality.

Signed by the final Examining Committee:

_____ Chair
Aashiq H. Kachroo, PhD

_____ External Examiner
David H. Kwan, PhD

_____ Examiner
Vincent Martin, PhD

_____ Supervisor
Christopher L. Brett, PhD

Approved by _____
Grant E. Brown, PhD
Graduate Program Director

February 8th, 2024 _____
Pascale Sicotte, PhD
Dean of the Faculty of Arts and Science

Abstract

Exploring protein candidates with enhanced cargo loading capabilities into *Saccharomyces cerevisiae* extracellular vesicles

Alexander Christophe Pawelczak

Extracellular vesicles (EVs) are a promising drug delivery platform as they compartmentalize bioactive payloads prior to delivery, have low immunogenicity, and are capable of tissue-specific targeting. EV-based therapeutics in most research pipelines are produced using cultured human mesenchymal stem cells. This approach is limiting as they are not amenable to complex genetic engineering, are expensive to grow and maintain, produce heterogenous EVs that are challenging to purify, and cannot be easily upscaled. Baker's yeast (*Saccharomyces cerevisiae*) is an excellent candidate for EV research, as it exhibits similar fundamental EV biology and may overcome these and other limitations. Using *S. cerevisiae* as a model, this study aims to determine if yeast strains expressing EV localization peptides can produce engineered EVs loaded with bioactive cargo. To achieve this, a panel of genetically modified yeast strains was generated to express fluorescently tagged versions of known EV markers and bioproduction was quantified with single particle analyses.

Acknowledgements

To my supervisor, Dr. Christopher Brett, I would like to express my gratitude for your unwavering support and mentorship throughout this study. It was an immense privilege to learn from your expertise and I recognize that this experience has enabled me to expand my knowledgebase and skillset and grow as a scientist. I would also like to thank my committee members Dr. Vincent Martin and Dr. Aashiq Kachroo for their research insight and support during this project.

I would like to thank my colleagues Dr. Jeff Bouffard, Devina Singh, Curt Logan and Joseph Trani for being there to help me learn, as well as other members of the Brett lab and the Biology department who have offered their guidance and friendship. You have provided a sense of community and made my time here memorable. To Christien and Derin, you have been present for the highs and the lows and I will never forget how much you have made this journey enjoyable. The dedication and passion you have towards your work is truly inspiring and I have no doubt that you will reach great heights.

I thank Dr. Chris Law, the operations manager and microscope specialist of the Centre for Microscopy and Cellular Imaging at Concordia University for sharing his technical skills with me. To Dr. Nadim Tawil and Hélène Pagé-Veillette from the Centre of Applied Nanomedecine at the Research Institute of the McGill University Health Centre, I would like to thank you for technical support in single-particle analysis and your guidance. I would also like to thank Angela Quach from the Concordia Genome Foundry for her training on flow cytometry and troubleshooting tips.

Additionally, I thank the NSERC CREATE Synthetic Biology Applications program and the program manager Orly Weinberg for the support and exceptional training I was provided with throughout my degree.

Finally, I would like to thank my family and my partner – this would not have been possible without your love and support.

Author Contributions

Table 1. Dr. Jeff Bouffard generated the plasmids and strains listed.

Figure 2. Dr. Jeff Bouffard provided illustrations A and B.

Figure 6. Curtis John Logan acquired the TEM images shown.

All authors reviewed the final manuscript and approved of the contents.

Table of Contents

LIST OF FIGURES

LIST OF TABLES

List of abbreviations

DPBS	Dulbecco's phosphate buffered saline
DIC	differential interference contrast
ECM	extracellular matrix
ESCRT	endosomal sorting complexes required for transport
EV	extracellular vesicle
GFP	green fluorescent protein
ILV	intralumenal vesicle
MFI	mean fluorescence intensity
MHC	major histocompatibility complex
MV	microvesicle
MVB	multivesicular body
OD_{600}	optical density at 600 nm
PBS	phosphate buffered saline
SC	synthetic complete
SEM	standard error of the mean
TEM	transmission electron microscopy
TIRF	total internal reflection fluorescence
VPS	vacuole protein sorting

CHAPTER 1 INTRODUCTION

1.1 An overview of extracellular vesicle discovery

All organisms interact with their environment and other individuals through the exchange of chemical signals, allowing them to develop, respond to stimuli, and maintain homeostasis. This complex interchange of information can be mediated by extracellular vesicles (EVs) that compartmentalize bioactive cargoes prior to being released by cells, which subsequently circulate through the extracellular space. When internalized by recipient cells, EV payloads can be delivered to the cytosol, triggering a wide range signaling events (van Niel et al., 2022). The term EV refers to diverse populations of lipid nanoparticles that can be released by virtually all cells, and vary in terms of size, surface composition and lumenal cargoes depending on the producing cell type and its metabolic state (Dixson et al., 2023). In the field of EV biology, it is recognized that there are two major classes of vesicles consisting of exosomes and ectosomes. The former is produced from the endocytic pathway through which the coordinated activities of the endosomal sorting complexes required for transport (ESCRTs) generate intralumenal vesicles (ILVs) that undergo exocytosis. The latter refers to particles ranging from 100 – 1,000 nm in size generated from outward protrusions of the plasma membrane that are excised, and subsequently shed into the extracellular space (Teng and Fussenegger, 2021).

The history of EV discovery is one of gradual developments and paradigm shifts spanning multiple decades, showcasing how a biological process with seemingly little functionality became recognized as one with far-reaching implications. In the mid-20th century, prior to being recognized as biological entities, EVs were first described as pro-coagulant factors separated by ultracentrifugation (Chargaff and West, 1946). In the 1980s, Johnstone's work demonstrated how the release of exosomes were involved in downregulating the transferrin receptor within maturing sheep reticulocytes and provided evidence for their involvement in membrane trafficking (Johnstone et al., 1987). However, these findings and the works of others contributed to the prevailing misconception regarding EVs, characterizing them merely as a waste disposal mechanism, discouraging exploration in their biological significance (Johnstone et al. 1991). During this period, the groundwork for understanding the prevalence of EV

secretion across microorganisms was laid through investigations on non-mammalian species. For instance, it was shown that *Ochromonas danica* secretes a range of vesicles capable of being isolated via centrifugation, and EV preparations released from *Candida tropicalis* could delay the growth of other yeast cultures (Aaronson et al., 1971; Chigaleĭchik et al., 1977). Vesicles released from *Corynebacterium* were shown to induce cell agglutination, and EVs secreted by *Acinetobacter* were shown to possess lipopolysaccharide complexes (Vysotskiĭ et al., 1977; Käppeli and Finnerty, 1979). These early studies contributed to our understanding of the ultrastructural characteristics of EVs and provided evidence for their mechanisms of release to be conserved across multiple domains of life. It was not until the beginning of the millennium where the field of EV biology experienced a remarkable surge in interest due to pivotal studies demonstrating the role of EVs in intercellular communication and immunity, and their recognition as biomarkers for altered physiological states (Ratajczak et al., 2006; Skokos et al., 2003; Wolfers et al., 2001). The field witnessed its first EV meeting in 2000 and founded the International Society of Extracellular Vesicles in 2012, bringing together researchers to explore various disciplines in EV biology, address standardization and reporting, and tackle technical challenges (Couch et al., 2021). Today, there continues to be a growing community of researchers exploring the nature of EVs which has led to the formation of National Societies found globally. The tremendous growth in interest and research output has allowed EVs to be viewed as clinically relevant, driving a community of researchers to better understand their biogenesis, the mechanisms underlying their functional transfer of cargo, and their broad therapeutic applications.

1.2 EV biogenesis

In order to fully harness the clinical capabilities of EVs, we must understand the processes governing their composition, and the pathways underlying their secretion. Elucidating these may provide candidate proteins suitable for engineering therapeutic EVs. However, this has been a major challenge in the field as subpopulations of EVs may be difficult to distinguish due to overlapping characteristics relating to their size and cargoes. Current EV purification techniques fail to produce monogenic preparations which hinders our ability to properly

differentiate EV subtypes. Nevertheless, membrane trafficking is a heavily researched topic and researchers have been able to elucidate different EV biogenesis pathways. In the literature, small EVs (or exosomes) have been associated with the ESCRT-dependent route of biogenesis (Dixson et al., 2023).

1.2.1 ESCRT – dependent EV biogenesis

Exosomes (small EVs) represent a class of EVs that is most abundant in biological fluids (Buzas, 2023). Though their biogenesis has not been fully elucidated, studies have established that their production is mainly driven by a series of sequentially acting conserved protein complexes termed ESCRTs (Henne et al., 2011). They are involved in the maturation of the endosome by coordinating its transition to a multivesicular body which has been initially observed in yeast. This entails that portions of the limiting membrane invaginate and bud into the lumen of the endosome, forming ILVs that sort lipids and transmembrane proteins. This mechanism begins when ESCRT-0 recognizes and binds to ubiquitinated cargo on the cytosolic face of the endosome initiates their sorting to MVBs. ESCRT-I is recruited and binds to both ESCRT-0 and to ubiquitinated cargo proteins which allows for the progression of the ESCRT pathway. ESCRT-II is subsequently recruited and initiates the formation of the ESCRT-III complex, driving the final stages of ILV formation. Stabilized by Bro1, ESCRT-III mediates cargo packaging and membrane deformation while the accessory protein Doa4 removes ubiquitin from the cargo. The ATPase accessory protein complex Vps4 is recruited, driving vesicle scission and the release of ESCRT complexes, resulting in ILV formation within the endosome. Mature MVBs subsequently fuse with the plasma membrane, releasing ILVs into the extracellular space **(Figure 1)**.

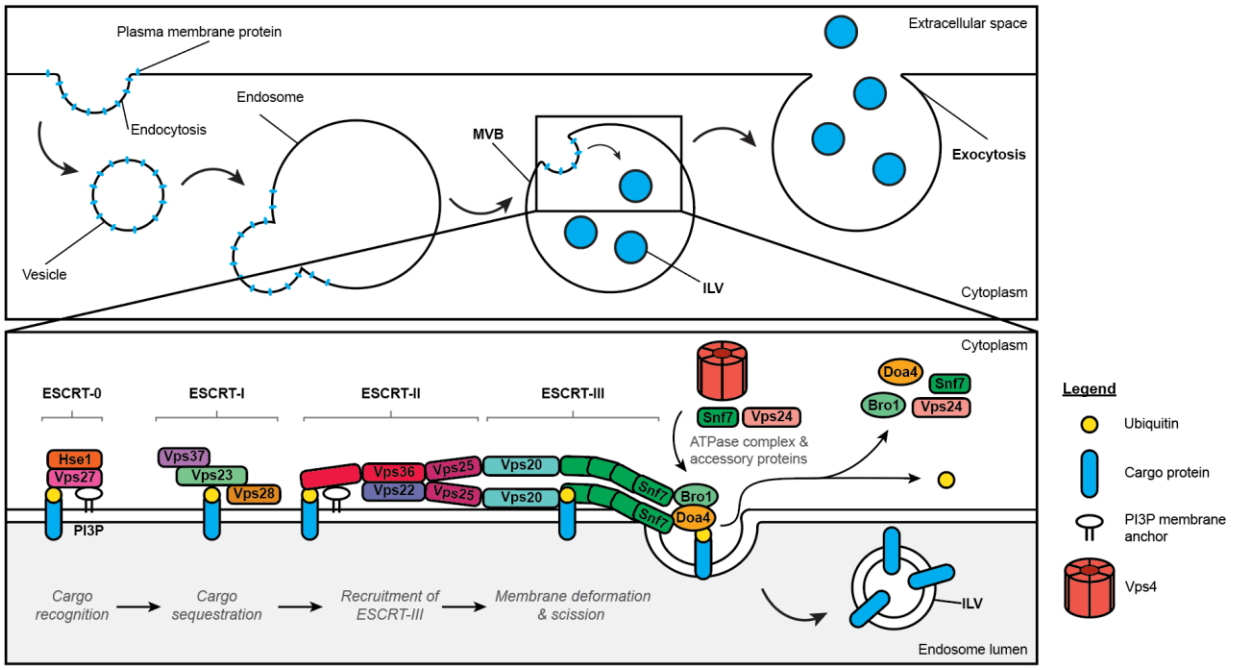

Figure 1. ESCRT-dependent exosome biogenesis

Ubiquitylated cell surface proteins undergo endocytosis, resulting in the formation of cytosolic vesicles that fuse with the endosome. ESCRTs are recruited to the cytoplasmic face of the endosome membrane to select and package proteins into ILVs. ESCRT-0 recognizes and binds to ubiquitylated proteins at the endosome membrane. Ubiquitylated proteins are sequentially transferred to ESCRT-I and ESCRT-II for cargo sorting. The cargo protein is transferred to ESCRT-III and accessory proteins Doa4 and Bro1. Packaging of proteins is performed via membrane deformation and scission, leading to the formation of ILVs. Prior to ILV release into the endosomal lumen, ESCRTs are disassembled by Vps4 and cargo proteins are deubiquitylated by Doa4. After multiple rounds of ILV formation, a mature MVB is formed. MVBs fuse with the plasma membrane, releasing ILVs as exosome into the extracellular space. Adapted from (Williams and Urbé, 2007; Saksena et al., 2007).

1.3 The role of EVs in physiology and disease

EVs are ubiquitous in nature as they are produced by organisms in of all domains of life and found in nearly all biological fluids of the human body (Pulliero et al., 2019). They represent an incredible means of intercellular communication capable of compartmentalizing biological cargoes such as proteins and nucleic acids, which in turn orchestrate diverse signalling pathways when delivered to recipient cells. As the field of EV biology witnessed a surge in growth, the research community has identified numerous homeostatic functions regulated by EVs. For instance, in the context of immunity, EVs released from thymic epithelial cells can regulate the development of lymphocytes by carrying tissue-restricted antigens to thymic conventional dendritic cells in order to promote central tolerance (Skogberg et al., 2015). Additionally, reports have shown that B-cell-derived EVs have the capacity to possess functional peptide-MHC complexes capable of activating T-cells through antigen presentation via direct or indirect mechanisms (Raposo et al., 1996; Théry et al., 2002; Utsugi-Kobukai et al., 2003). EV-associated proteins may promote wound-healing in damaged tissues that have been subjected to trauma, inflammation, infection, by preventing cell death, triggering neovascularization, and inducing cell proliferation (Zhang et al., 2015; Gong et al., 2019; Liu et al., 2020). Conversely, EVs have been increasingly implicated in disease progression. Cancers can mediate metastasis by secreting EVs that modify the metabolism of the tumor microenvironment. For example, in murine models, breast cancer cells secrete EVs that suppress glycolysis and insulin secretion, enabling their growth (Cao et al., 2022). Pancreatic cell-derived EVs carry out ECM remodelling while inhibiting the migration of bone-derived macrophages, resulting in premetastatic niche formation (Costa-Silva et al., 2015). EVs can additionally be involved in the progression of neurodegenerative diseases as they can disseminate pathophysiological proteins such as PrP^{Sc}, resulting in the development of Alzheimer's disease (Hartmann et al., 2017). These findings highlight how EVs are involved in broad (patho)physiological processes by initiating signaling pathways via the interaction of their surface proteins with recipient cells or by the delivery of intralumenal cargos. Hence, modifying components of EVs could be achieved in order to mediate physiological pathways for therapeutic purposes.

1.4 EV engineering strategies for therapeutic applications

Developing a strategy to deliver pharmaceutical agents safely and effectively to specific targets represents a major challenge in the generation of novel therapeutics. Currently, treatments for chronic illnesses can cause a range of intolerable effects in patients as a result of disrupting healthy physiological processes or causing immunogenic responses (Zahler et al., 2019). For instance, cytotoxic drugs used in chemotherapy regimens often exhibit a system-wide presence when administered. On top of producing negative side-effects, this phenomenon further reduces the effectiveness of treatments as this provides a greater opportunity for therapeutic agents to be degraded or metabolized prior to their delivery to targeted cells. This is a primary concern regarding other forms of treatments such as gene therapy, RNA silencing and enzyme replacement therapy. Different strategies have been developed to improve therapeutic delivery by utilizing synthetic nanocarriers such as liposomal and polymeric nanoparticles to administer a variety of therapeutic molecules. Both consist of synthetic compounds that have the ability to encapsulate drugs prior to their delivery (Gelperina et al., 2005). Despite their ability to stabilize drug molecules or provide a layer of protection, their use is associated with a number of drawbacks, which include (1) causing immunogenic and cytotoxic responses in subjects, (2) being limited in their efficacy to deliver therapeutics to target cells, (3) being unable to cross the biological barriers, and (4) possessing manufacturing challenges relating to quality control and cost (Bertrand and Leroux, 2012). EVs are better suited for drug delivery compared to synthetic nanoparticles since they possess traits that constitute the ideal drug delivery system. For instance, EVs are non-toxic and produce low to no immunogenic responses in hosts, which is attributed to their natural origin and their similarities to the cells of the body (Dang et al., 2020). Their surface proteins enable them to be internalized by multiple types of cells, as well as pass the blood-brain barrier and large tissues while avoiding bioaccumulation (Mulcahy et al., 2014; French et al., 2017). EVs have been harnessed for clinical therapy by applying different engineering approaches involving genetically modifying parental cells or altering EVs post-isolation.

1.4.1 Enhancing stealth properties and targeted tissue homing

There are currently a number of known strategies being applied to increase the therapeutic value of EVs. A major challenge regarding the application of EV-based therapeutics involves preventing the engulfment of particles by off-target hepatic and splenic macrophages of the reticuloendothelial system (Wiklander et al., 2015). Modifying the surface of EVs to increase their stealth properties and organotropic homing effects for improving biodistribution and cell targeting is a promising strategy to increase their therapeutic efficiency. The presence of CD47 can suppress exosome clearance by monocytes, resulting in increased pancreatic tumor suppression and survival in mice (Kamerkar et al., 2017). EVs can be further "cloaked" with tissue targeting peptides using a chemical membrane anchor and a conjugated streptavidin platform molecule where homing molecules can be bound. This technology has been applied for increasing exosomal uptake in healthy and injured cardiac tissues, and could be applied to enhance targeting in lung, brain, kidney and muscle tissues using known homing peptides (Johnson et al., 1993; Ghosh and Barry, 2005; Denby et al., 2007; Li et al., 2012; Antes et al., 2018). Increasing targeting efficiency can also be achieved by expressing recombinant proteins in EV-producing cell lines comprising of a homing peptide with membrane binding domains commonly associated with EVs. This strategy has been applied for targeting $HER2^+$ breast cancer by fusing a high-affinity anti-HER2 scFv antibody to the C1C2 domain of lactadherin (Delcayre et al., 2005; Wang et al., 2018). The most straightforward strategy consists of modifying parental cell lines expressing recombinant homing peptides bound to EV-enriched transmembrane proteins as this minimizes the extent of genetic modification. Both CD63 and the PDGFR transmembrane domain (common EV markers in mammalian cells) have been utilized in this fashion to enhance the drug delivery of anticancer molecules to mantle cell lymphoma, and to perform targeted breast cancer immunotherapy (Bao et al., 2017; Shi et al., 2020; Jayasinghe et al., 2021). These results showcase how there are promising strategies being developed in order to overcome the limitations of EV-based therapeutics involving targeted tissue delivery.

1.4.2 Cargo loading

One of the main approaches involved in developing EV-based next generation therapeutics involves the encapsulation of therapeutic molecules. Different engineering strategies

are employed depending on the type of cargo one desires to incorporate. To deliver soluble peptides via EVs, parental cell lines can be genetically modified to express proteins that may be packaged into vesicles prior to their externalization. This strategy can be further applied to deliver RNA in recipient cells that will manufacture a functional therapeutic protein, or silence gene expression (Kamerkar et al., 2017; Yang et al., 2020) To enhance the loading of protein in EVs, a viable strategy would involve a similar technique mentioned above where parental cell lines express recombinant proteins bound to known EV markers that localize in the EV lumen rather than its surface. There is a growing number of known EV sorting proteins available that can be incorporated to produce more efficient engineered EV-based therapeutics (Zheng et al., 2023). Encapsulating therapeutic molecules can be performed post-isolation via passive and active methods of loading. In a simple manner, molecules with poor solubility can be incorporated into EVs via coincubation (Haney et al., 2015). There are a variety of substances that can be packaged using this method ranging from dietary supplements to chemotherapeutic agents, which demonstrate a loading efficiency dependent on the extent of their hydrophobicity (Sun et al., 2010; Fuhrmann et al., 2015). Encapsulating small hydrophilic molecules such as nucleotides is commonly achieved via electroporation (Jayasinghe et al., 2021). The administration of high-voltage pulses generates transient pores that facilitate the diffusion of nucleotides through the EV bilayer (Kooijmans et al., 2013). However, this method may cause particles to aggregate and could require optimization depending on the molecule of choice (Stoicheva and Hui, 1994; Wang et al., 2018). Nonetheless, the use of electroporated EVs has been demonstrated to deliver antisense oligonucleotides, Cas9 mRNA and gRNAs to recipient cells with a higher efficiency in comparison to commercial transfection agents (Usman et al., 2018).

1.4.3 Industry trends for EV-based therapeutic technologies

Designer EVs can allow clinicians to implement a safer, more target specific and far-reaching drug delivery platform. So far, the majority of the therapeutic applications mentioned here involved the treatment of various cancers. However, many groups have recently harnessed EVs to treat broad clinical manifestations. For instance, this technology is being developed for

novel regenerative therapies. Engineered EVs have the capacity to mediate wound healing in organotypic full-skin models and treat myocardial ischemia-reperfusion injury in mice (Staufer et al., 2021; Wei et al., 2019). Notably, this technology has been applied to elicit functional recovery in rats exhibiting complete spinal cord injury (Guo et al., 2019). EVs are being further implemented as vaccines against SARS-CoV-2, for the attenuation of inflammation, and as cosmeceutical agents for facial aesthetics (Harrell et al., 2019; Wang et al., 2022; Lee et al., 2020).

The beginning of the millennium marked a surge in growth in the field of EV research. Between the years of 2009 and 2018 there has been 733-fold increase in EV related publications per year, and today, there are over 500 US patents filed, which include the term EV (Couch et al., 2021; Song et al., 2021). The abundance of evidence highlighting the potential EVs offer as a novel drug delivery platform has resulted in the emergence of a new synthetic biology sector where private entities are developing designer EV therapeutics for clinical use. As the industry is still in its infancy, there are currently no engineered EV therapies available. However, the market is poised for growth with revenue projected to double in 2026 from USD 170 million in 2020 (Pirisinu, 2023). It is worth noting that this sector is just one branch of a larger industry projected to be valued at USD 1.03 billion by 2030 which further encompasses companies developing EV-based analysis and diagnostic services, and EV isolation kits and reagents (Research and Markets, 2023). Current research pipelines involve the development of designer EVs for gene therapy, treatment for Duchenne muscular dystrophy, therapies for neurological disorders and dermal tissue damage.

1.5 *S. cerevisiae* as a platform for engineered EV production

Strides have been made in developing engineered EVs for targeted therapies, but challenges delay their commercial viability. The reason for this is that most research pipelines use human mesenchymal stem cells, which have (1) low biomanufacturing output, (2) have high growth and maintenance cost, (3) are not amenable to complex genetic engineering, and (4) have the capacity to release components of stemness (Gowen et al., 2020; Wiest and Zubair, 2020).

These limitations highlight the need for an alternative manufacturing platform to realize the therapeutic potential of EVs. However, EV function is not limited to humans. They perform important physiological roles in all organisms, including baker's yeast (Oliveira et al., 2010). This powerhouse organism is extensively used in biomanufacturing, has unmatched genetic amenability and an incredible record of success in uncovering the basis of fundamental cellular processes (Bean et al., 2022; Lee et al., 2015; Thodey et al., 2014; Zimmermann et al., 2016). *S. cerevisiae* is also the model of choice to study orthology, revealing deep evolutionary conservation of essential pathways through ectopic expression of human genes in place of yeast counterparts (Kachroo et al., 2015; Kachroo et al., 2017). Thus, *S. cerevisiae* would be an exceptional platform to genetically engineer EVs for new applications, and to eventually manufacture EVs for use. The aim of this study is to determine the extent at which designed ExoTags localize to isolated yeast EVs. If the ExoTags are found to be abundant in EVs they could be used in downstream clinical applications for the purpose of cargo delivery and cell targeting **(Figure 2)**.

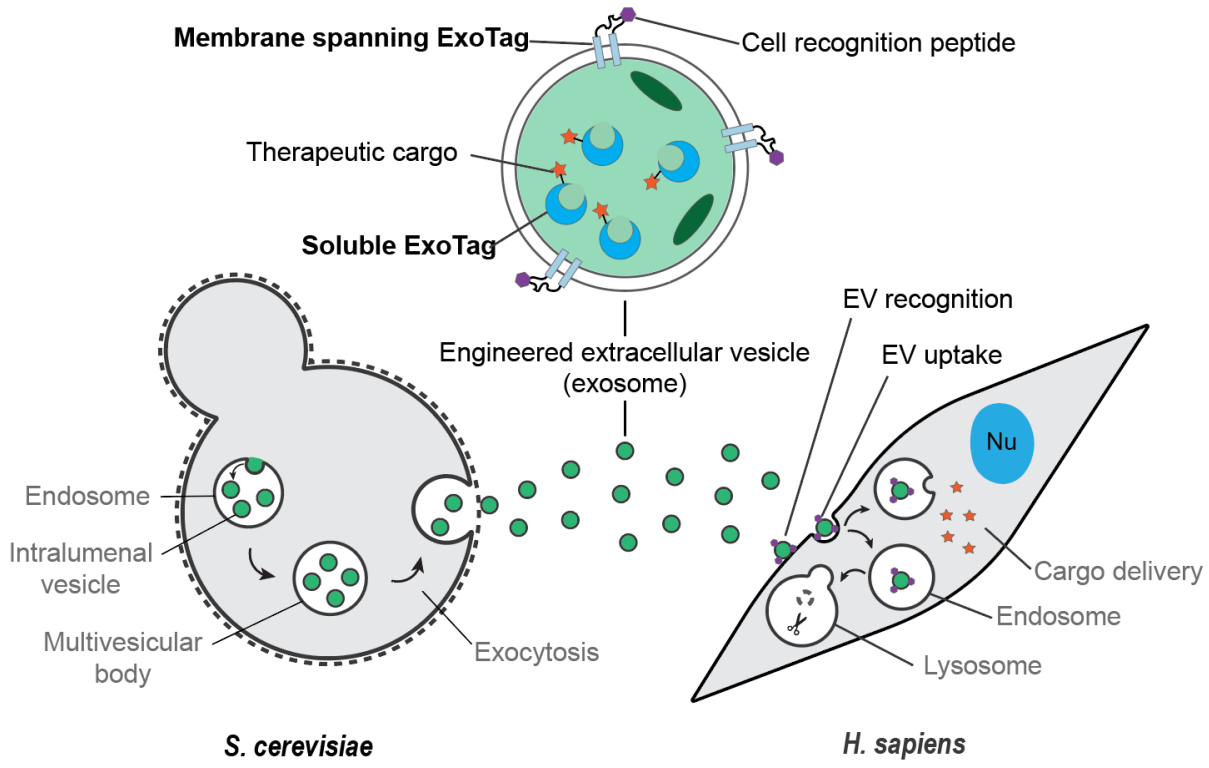

Figure 2. Engineered yeast EVs for enhanced cell recognition and cargo delivery

A cartoon representing the trafficking of engineered EVs from yeast to humans. Genetically modified *S. cerevisiae* is used to express soluble or membrane spanning EV localization signals (referred as ExoTags) fused with therapeutic cargo or cell-targeting peptides that may be incorporated into exosomes during their biosynthesis. Endosomes undergo maturation, which involves the inward budding of the endosomal membrane, forming intralumenal vesicles and results in a multivesicular body. The multivesicular body fuses with the cell's plasma membrane, releasing exosomes in the extracellular space. Engineered exosomes (i.e. those possessing ExoTags) can be used to enhance cell-specific targeting and internalization as well as delivering therapeutic cargo into human cells.

CHAPTER 2 MATERIALS AND METHODS

2.1 Yeast strains and reagents

The *Saccharomyces cerevisiae* background strain used in this study is BY4741 (MATa his3Δ1 leu2Δ0 met15Δ0 ura3Δ0). Reagents for yeast growth, EV isolation and imaging or biochemical assays were purchased from Thermo Scientific, BioShop Canada Inc., Invitrogen and Sigma-Aldrich.

2.2 Golden Gate and Gateway assembly for generating expression vectors

Expression vectors used in this study are listed in Table 1. Golden Gate reactions were prepared as follows: 75 ng of the backbone vector and 20 fmol of DNA insert, 1 µL T7 ligase (3x10^6 units/mL); (NEB; M0318S), 1 µL 10 mM ATP (ThermoFisher; PV3227), 1 µL of 10 U/µL restriction enzyme, 1 µL of 10X enzyme buffer and water to make a final volume of 10 µL. Each reaction mixture was incubated on a thermocycler with the following program: 30 cycles of digestion and ligation (37 ºC for 1 min, 16 ºC for 1 min) followed by a final digestion step (end-on-digestion at 37 ºC for 15 min) or with a final ligation step (end-on-ligation at 16 ºC for 60 min) and a heat inactivation step (85 ºC for 15 min).

Gateway cloning was performed as follows: 150 ng of DNA insert, 150 ng of destination or entry vector, 1X TE buffer (pH 8.0) were combined into a final volume of 8 µL. Subsequently, 1 µL of BP or LR clonase was added (Invitrogen; 11791020, 11789100). The reaction was incubated at room temperature overnight. The following day, 1 µL of Proteinase K (2 µg/µL) (Invitrogen; 11791020, 11789100) was added to the mixture to halt enzymatic activity. The reaction was transformed in ccdB sensitive DH5α *E.coli* competent cells and plated on LB agar with antibiotic selection. All plasmids were sequence-verified (Plasmidsaurus Inc., Oregon).

Table 1. Plasmids used in this study

Plasmid	Strain name	Description	Source
pBrett70	Exosignal	P_{TDH3}-*GFP*-Exosignal-T_{ADH1}, P_{URA3}-*URA3*-$T_{URA3,}$ 2μ, ColE1, P_{Ampr}-Amp^r-T_{Ampr}	This study
pBrett93	PDGFR	P_{TDH3}-*GFP-PDGFR-mRuby* -T_{ADH1}, P_{URA3}-*URA3*-$T_{URA3,}$ 2μ, ColE1, P_{Ampr}-Amp^r-T_{Ampr}	This study
pBrett40	CD63 full-length	P_{TDH3}-*mRuby-HsCD63-GFP*-T_{ADH1}, P_{URA3}-*URA3*-$T_{URA3,}$ 2μ, ColE1, P_{Ampr}-Amp^r-T_{Ampr}	This study
pBrett38	CD63 C-term	P_{TDH3}-*mRuby-HsCD63 C-term-GFP*-T_{ADH1}, P_{URA3}-*URA3*-$T_{URA3,}$ 2μ, ColE1, P_{Ampr}-Amp^r-T_{Ampr}	This study
pBrett106	GFP-Bro1	P_{TDH3}-*GFP-BRO1*-T_{ADH1}, P_{URA3}-*URA3*-$T_{URA3,}$ 2μ, ColE1, P_{Ampr}-Amp^r-T_{Ampr}	This study
pBrett107	Bro1-GFP	P_{TDH3}-*BRO1-GFP*-T_{ADH1}, P_{URA3}-*URA3*-$T_{URA3,}$ 2μ, ColE1, P_{Ampr}-Amp^r-T_{Ampr}	This study

2.3 Yeast transformation

BY4741 was inoculated in 5 mL YPD. Yeasts were then back diluted and incubated for 4 hrs or until they had an OD_{600} of 0.8. Yeasts were pelleted and washed twice (3,500 RPM, 3 min) in 1X TE (1 nM EDTA, 10 mM Tris, pH 7.5). Next, pellets were resuspended in 0.1 M LiOAc and were incubated at room temperature for 1 hr. Supernatants were then transferred to a 1.5 mL Eppendorf tube and pelleted (10,000 RPM for 30 sec). After discarding the supernatant, the pellet was suspended in 34 μL sterile water, 10 μL ssDNA, 10 ng amplicon or plasmid DNA, 36 μL 1 M LiOAc, and 240 μL PEG (50% PEG3350, 0.1 M LiOAc, 1 nM EDTA, 10 mM Tris, pH 7.5). This solution was allowed to incubate at room temperature for 1 hr. Next, 36 μL of DMSO was added to this solution, with the entire cell suspension being subsequently heat shocked for 5 min at 42 ˚C. The cell suspension was then allowed to rest at room temperature for 5 min, with the pellet being subsequently collected (10,000 RPM for 30 sec). The pellet was suspended in sterile water and plated on the appropriate selection.

2.4 Strain establishment by flow cytometry

The percentage of GFP^+ cells and mean fluorescent intensity (MFI) were measured using a BD FACS Melody (BD Bioscience, Canada). The FACS was equipped with three excitation lasers (405, 488, and 561 nm) in a 2B-2V-4YG configuration. For all experiments, cells were grown overnight in 5 mL of SC (for WT) or SD -Ura (for modified strains) from a glycerol stock. The OD_{600} was measured, and 5 OD units of cells were captured and DPBS was added up to final volume of 5 mL. Samples were washed by centrifuging (1000 g, 3 min), aspirating the supernatant and suspending in 5 mL DPBS. The sample was centrifuged once more and cells were suspended in 1 mL DPBS. Cells were excited by a 488 nm laser and viewed through a 527/32 filter. The cell populations were used to generate a histogram showing GFP expression. For each condition, 100,000 events were collected. Analysis and figure preparation were performed using Floreada.io (last updated on 8/12/23).

2.5 Live-cell fluorescence microscopy

To confirm the expression of fluorescently labeled recombinant proteins by transformed *S. cerevisiae* in-vivo, cells were grown in 5 mL media (SC-URA) at 30 ˚C, shaking at 200 rpm for 24 hrs. The OD_{600} values of cultures were measured, and 5 OD units of cells were harvested by centrifugation at 3500×g for 1 min, washed, and suspended in 100 µL of PBS. Following this, 10 µL of suspended cells were transferred to glass slide, covered with glass coverslips, and imaged via a Nikon Eclipse TiE inverted microscope equipped with a motorized TIRF (Total Internal Reflection Fluorescence) 13 illumination unit, Photometrics Evolve 512 EMCCD (Electron Multiplying Charge Coupled Device) camera, Nikon CFI ApoTIRF 1.49 NA × 100 objective lens, and 488 nm or 561 nm 50 mW solid-state lasers operated with Nikon Elements software. The expression of fluorescent labels was visualized in ≥ 3 biological replicates per strain.

2.6 EV isolation by ultrafiltration

Yeast glycerol stocks were inoculated into 15 mL of liquid media (SC or SD-URA) and grown at 30 ˚C and 200 rpm for 36 hrs. For each strain, pre-cultures were inoculated into three 2 L flasks containing 1 L of media and grown overnight at 30 ˚C and 200 rpm until the cultures reached an OD_{600} value of 8 – 10 arbitrary units. Yeast cells were harvested at 4,000 rpm for 10 min and pellets were washed twice with phosphate buffered saline (PBS, pH 7.4). The pellets were subjected to 15 min of heat stress at 42 ˚C, suspended in 25 mL of Dulbecco's phosphate buffered saline (HyClone DPBS, Cytiva) and incubated at 42 ˚C for an additional 15 min. The cell suspension was centrifuged at 5,000×g for 15 min at 4 ˚C, the supernatant was collected and centrifuged at 15,000×g for 15 min at 4 ˚C and the supernatant was filtered (0.22 μm pore size, Corning Inc.). The filtered supernatant was subjected to ultrafiltration with centrifugal filter units (Amicon Ultra-15 NMWL of 100 kDa, MilliporeSigma) by centrifugation at 3700 rpm for a duration of 1 min/mL. EVs were collected from the filter unit and stored on ice for further characterization. The protein concentration of EV samples was determined by Bradford assay, using bovine serum albumin (BSA) to generate standard curves and the absorbance was measured at 595 nm using a multimode plate reader at gain 110 (Synergy H1, Biotek). EV isolations as well as Bradford and fluorometry assays were performed ≥ 3 biological replicates per strain.

2.7 EV characterization by nanoparticle tracking analysis (NTA) and nano-flow cytometry

To measure particle size and concentrations, I performed nanoparticle tracking analysis (NTA) using a ZetaView nanoparticle tracking analysis instrument (Particle Metrix, Ammersee, 35 Germany) with software version 8.0.5.14 SP7. EV samples were diluted between 1:100 to 1:5000 in sterile DPBS in order to capture between 50 – 200 particles per frame. One mL of diluted EV samples were manually loaded with a 1 mL syringe and samples were slowly injected until conditions appeared optimal for acquisition. ZetaView instrument settings were as follows: Temperature (25 ˚C), laser λ (488 nm), filter λ (scatter) sens (75), shutter (100), FR (30), and 40 trace length (15). Between each sample, the instrument was flushed with at least 1.5 mL of DPBS. Unless otherwise reported, EV samples from ≥ 3 different yeast cultures (biological replicates) were examined.

Nano-flow cytometry was performed using the CytoFLEX system (Beckman Coulter, Pasadena, CA) equipped with two lasers (405 and 488 nm). The 405 nm violet laser was selected for side scatter (SSC) analysis with 1800 of manual threshold setting in the violetSSC-height (violetSSC-H) channel and gain set at 100 of violetSSC-H signal in the acquisition mode. Samples were loaded and run with slow flow rate (10 µl/min) for 3 min. Data were acquired and presented using CytExpert 2.0 software (Beckman Coulter). EV mean fluorescence intensity was determined. EV samples from ≥ 3 biological replicates were examined.

2.8 Transmission electron microscopy

EV samples were fixed by diluting them 1:1 with 2.5 % glutaraldehyde in 0.1 M sodium cacodylate. Fixed EVs (5 µL) were then dropcast onto glow discharged carbon–coated grids and allowed to absorb for 5 min at room temperature. EV–bound grids were washed twice with glycine and then rinsed four times with ultrapure pure water. Mounted EVs were then negative stained with 1 % phosphotungstic acid (1 min, room temperature), blotted with filter paper and dried (1 hr, room temperature). Grids were then imaged at 80–120 kV using a Talos L120C transmission electron microscope (Thermo Fisher Scientific, Toronto, Canada). Each sample was imaged once.

2.9 Data analysis and presentation

Micrographs were processed using ImageJ and Adobe Photoshop CC software. Images presented were adjusted for brightness and contrast and inverted.

CHAPTER 3 RESULTS

3.1 Generating engineered yeast strains for enhancing EV cargo loading

3.1.1 Cloning strategy and selected ExoTags

Compartmentalizing bioactive cargos in EVs is a major challenge in the field of nanobiology having many implications regarding the treatment of chronic illnesses in clinical settings. The objective of this study was to engineer endogenous EVs isolated from a panel of six genetically modified *S. cerevisiae* strains that constitutively express the following markers bound to a fluorescent reporter, which would naturally localize to EVs: (1) the KFERQ motif (Exosignal) which is found in proteins loaded into a subpopulation of exosomes, (2 & 3) the BRO1 accessory protein involved in exosome biogenesis and the yeast ortholog to the human ALIX protein known as an established EV marker (Bro1-GFP & GFP-Bro1), (4) the PDGFR transmembrane domain, shown to be useful in achieving EV surface display, which was codon-optimized, (5) the established EV marker CD63 (CD63 full-length) and (6) its C-terminal transmembrane domain (CD63 C-term) (Ferreira et al., 2022; Krylova and Feng, 2023; Hoshino et al., 2020; Ohno et al., 2013; Shi et al., 2020; Andreu and Yáñez-Mó, 2014; Stickney et al., 2016). As the presence of these markers in exosomes has been demonstrated in mammalian cell lines, it was hypothesized that their implementation for yeast EV engineering would be useful as their biogenesis is conserved.

To streamline the production of engineered EVs, we employed a modular genetic toolkit, EVClo, designed in-house. This method harnesses the power of Golden Gate and Gateway cloning in order to express human and yeast cDNAs under the strong constitutive yeast TDH3 promoter from a plasmid **(Figure 3A)**. Golden Gate assembly allows for the single-pot, scarless and directional assembly of multiple genetic components into a single vector via the ligation of matching overhangs (Andreou and Nakayama, 2018). The system designed for this study was built with to be compatible with the yeast toolkit, which categorizes genetic parts based on their function. Each part type is designated by predefined flanking overhangs, allowing the interchangeability of genetic components (Lee et al., 2015). The features that distinguish the

EVClo toolkit from regular Golden Gate assembly are (1) the BbsI site, which facilitates the incorporation of different ExoTags on individual vectors, and (2) a Gateway cloning cassette to fuse test cargos to ExoTags. The BbsI site is not a feature of the yeast toolkit. It is a component that was integrated in order to include an ExoTag to an assembled cassette plasmid, eliminating the need to reconstruct it anew. The Gateway cassette allows for the implementation of test cargo to plasmids based on the activity of clonase, an enzyme that recombines DNA fragments within specific sites of integration and excision (Reece-Hoyes and Walhout, 2018). Gateway cloning was implemented in order to utilize cDNAs from the human ORFeome collection housed in the Kachroo lab, which are flanked by Gateway cloning sites (Lamesch et al., 2007). Both of these characteristics increase the efficiency of strain generation by allowing for the rapid and modular alteration of EVClo constructs. The pipeline for building EVClo plasmids can be summarized as followed: (1) BsaI assembly is performed to build cassette plasmids from part plasmids, which contain an assembly connector, a promoter, a Gateway cassette, a terminator, a second assembly connector, a yeast marker, a yeast origin or replication and a bacteria marker and origin of replication. Then, (2) BbsI assembly is performed to integrate an ExoTag between the promoter and the Gateway cassette of the plasmid and (3) Gateway cloning is accomplished to fuse test cargo with the ExoTag. The power of this toolkit lies in its simplicity and amenability to batch cloning reactions for the systematic generation of engineered EV producer strains. In order to determine the efficiency of cargo loading from EV markers, the fluorescent tag GFP was fused to candidate proteins. The extent of GFP localization to EVs would be relative to the efficiency of the ExoTag **(Figure 3 B, C)**.

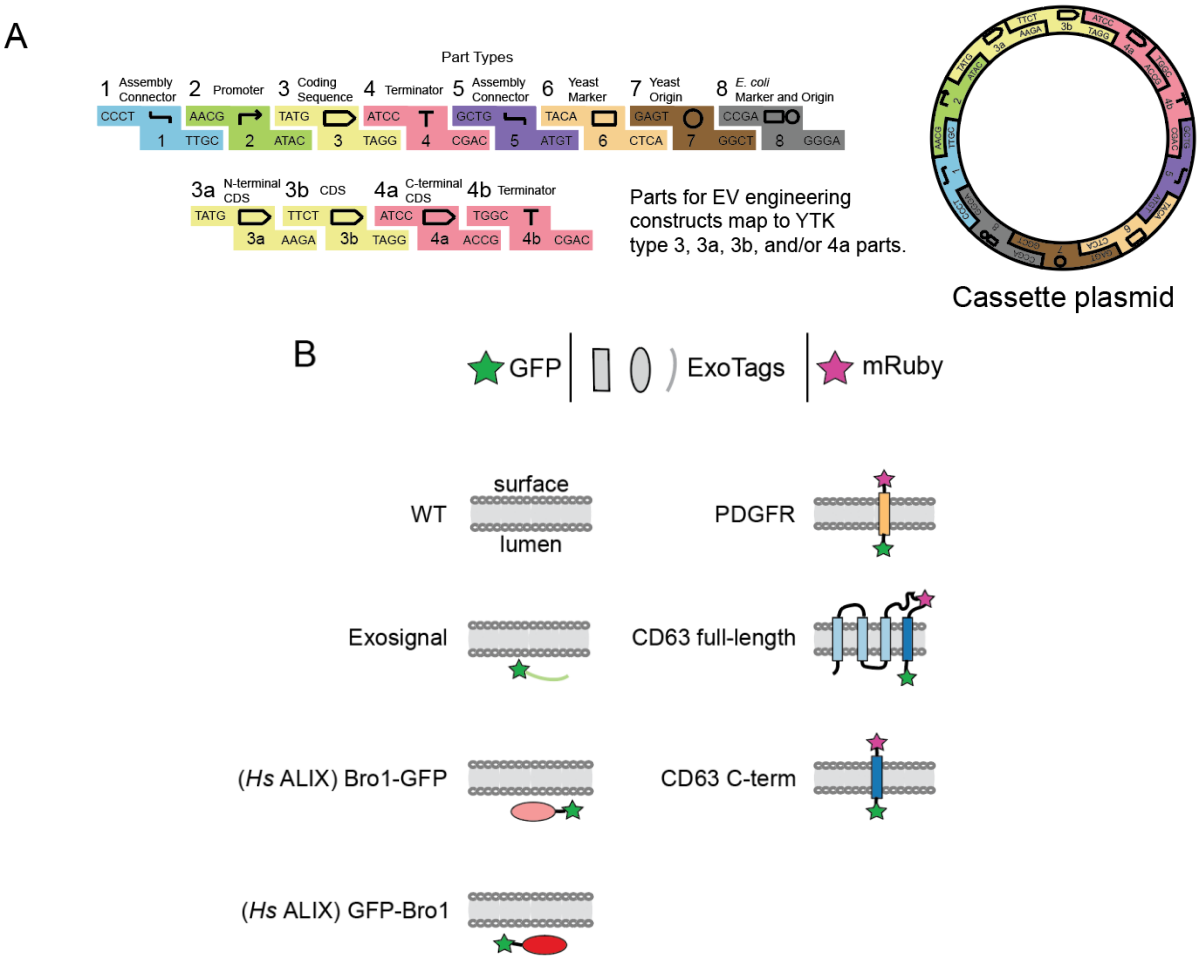
A
Part Types
1 Assembly Connector
2 Promoter
3 Coding Sequence
4 Terminator
5 Assembly Connector
6 Yeast Marker
7 Yeast Origin
8 E. coli Marker and Origin
CCCT
AACG
TATG
ATCC
GCTG
TACA
GAGT
CCGA
1 TTGC
2 ATAC
3 TAGG
4 CGAC
5 ATGT
6 CTCA
7 GGCT
8 GGGA
3a N-terminal CDS
3b CDS
4a C-terminal CDS
4b Terminator
TATG
TTCT
ATCC
TGGC
3a AAGA
3b TAGG
4a ACCG
4b CGAC
Parts for EV engineering constructs map to YTK type 3, 3a, 3b, and/or 4a parts.
Cassette plasmid
B
GFP
ExoTags
mRuby
WT
surface
lumen
PDGFR
Exosignal
CD63 full-length
(Hs ALIX) Bro1-GFP
CD63 C-term
(Hs ALIX) GFP-Bro1
C
CD63-C
CD63-N
GFP
Gateway cloning site
CD63-N
mRuby
CD63-C
GFP
EV producer (EV-Pro) strain
attB1-mRuby-attB2
C-term CD63
GFP
ADH1 term
URA3
2μ
TDH3 prom
N-term CD63
Transformation
S. cerevisiae
MVB
ExoTag
mRuby
GFP
Engineered S. cerevisiae EV

Figure 3. A platform for engineered EV bioproduction in *Saccharomyces cerevisiae*

(A) A representation of the characterized parts of the yeast toolkit for modular assembly and how EV parts readily fit into the system. YTK part types are categorized based on their functions in a plasmid and can be directionally assembled with complementary overhangs. Parts for EV engineering constructs could readily fit into this system as fluorescent proteins, Gateway cassettes and ExoTags. Adapted from (Lee et al., 2015). **(B)** A cartoon illustrating soluble and membrane spanning ExoTags fused to their cargos and where they are expected to localize on EVs. The membrane bilayer separates the contents of EVs from the exterior. Exosignal, and Bro1 are soluble ExoTags which should be present within the lumen of EVs. PDGFR, CD63 full-length and CD63 C-term would be membrane spanning ExoTags capable of presenting cargos on both the surface and lumen of EVs. **(C)** A schematic of EVClo to generate a four-component system for engineering EVs. This includes the N-terminal component of the ExoTag that was incorporated into the cassette plasmid via a BbsI Golden Gate reaction, a Gateway cloning cassette, the C-terminal component of the ExoTag and GFP. A gene expressing cargo for EV surface display is incorporated into the cassette plasmid via Gateway cloning. In this scenario the fluorescent reporter mRuby is inserted. The vector can be transformed into yeast to express fusiogenic proteins for EV engineering.

3.1.2 Validating the expression of fusion constructs

Prior to analyzing EV preparations from each engineered cell line, the expression of recombinant proteins was confirmed via flow cytometry and total internal fluorescent microscopy. The former method would demonstrate the percentage of cells producing fluorescent reporters while the latter would provide evidence for their assortment into EVs. As exosomes localize to MVBs, we would expect to visualize fluorescent punctate structures in cells expressing EV markers. Indeed, all strains demonstrated the expression of the fluorescent protein with a range of 51.8 – 78.9% of GFP positive cells compared with WT exhibiting no GFP expression **(Figure 4A, B)**. The mean fluorescent intensity of engineered cells ranges from 4,690 – 50,035 AU **(Figure 4C)**. It is worth noting that these results may not accurately represent GFP expression in engineered strains as one would expect to see a normal distribution of counts associated with cells that do not express GFP, and another normal distribution representing those that do. In these results, the peaks have been shifted to right, showing an unlikely bimodal distribution of GFP^+ cells. Furthermore, micrographs demonstrated the presence of fluorophores and punctate structures in engineered cells and not WT **(Figure 5A, B)**. Here, fluorescence was exhibited in 17.5 – 35.9% of cells and punctae were seen in 8.8 – 35.7% of cells throughout all strains **(Figure 5C)**. These data suggested that the generation of engineered strains expressing ExoTags, which potentially sort cargo to exosomes was successful, prompting the pursuit for downstream EV analyses.

Here I performed bulk analysis of EV isolates by measuring their GFP intensity with fluorometry in order to further validate the expression ExoTags. I anticipated that EVs isolated from engineered cell lines would exhibit higher fluorescence intensity as a result from ExoTag-mediated GFP sorting to EVs. Indeed, genetically modified yeast cells released EVs with higher fluorescence intensity in comparison to WT EVs **(Figure 6)**. Additionally, throughout the panel, exosomes released from the Bro1-GFP and GFP-Bro1 strains exhibited the highest GFP fluorescence intensity. This could suggest that these ExoTags possess greater cargo-loading capabilities compared to the others tested in this study. However, determining this requires the characterization of EVs and analyzing isolates on a single-particle basis.

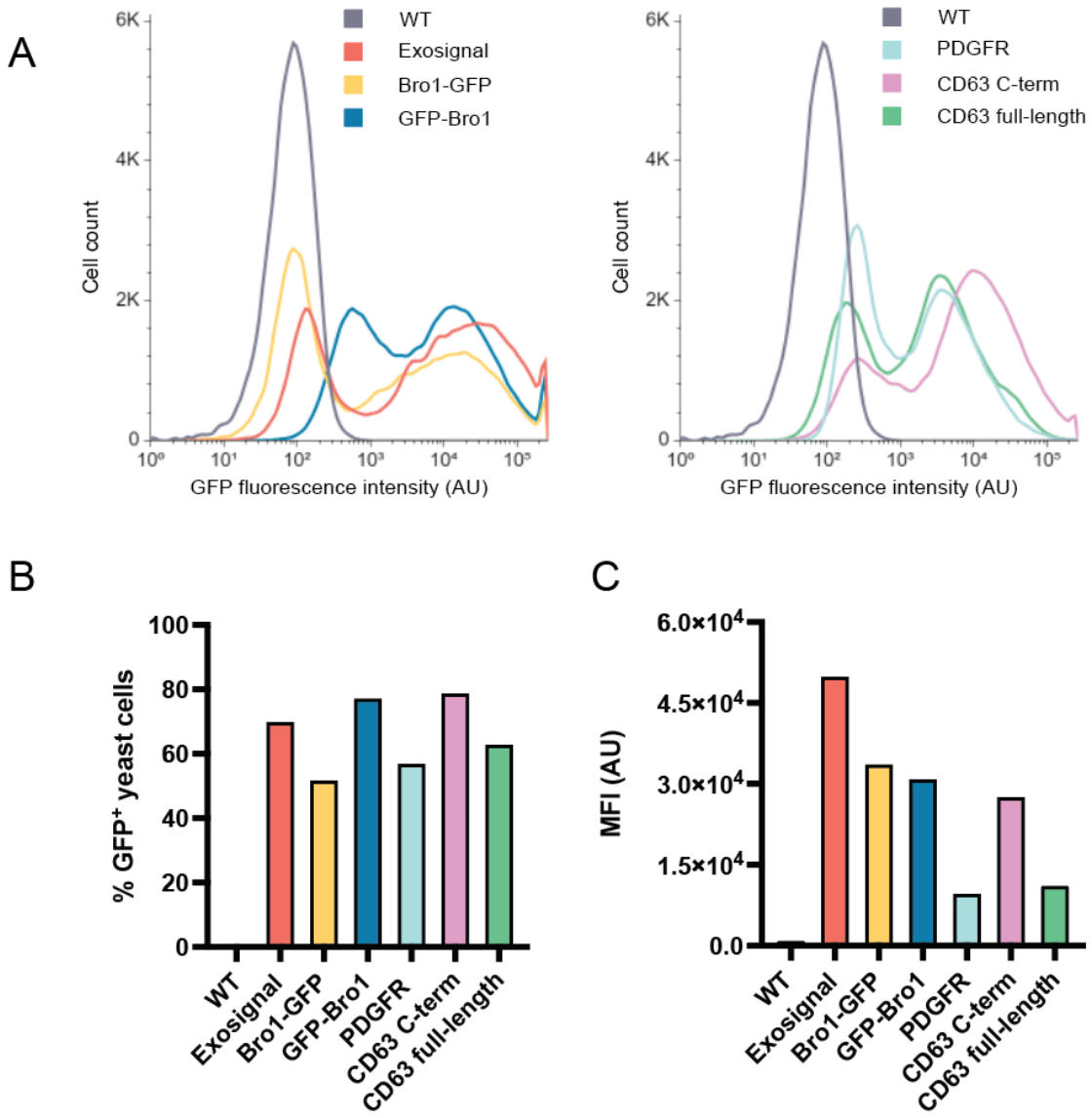

Figure 4. Strains express ExoTags built from the EVClo toolkit

(A) Histogram of genetically modified WT cells expressing ExoTags fused to GFP obtained via flow cytometry. GFP fluorescence intensity relative to number of events measured are shown (n=1). **(B, C)** The percentages of GFP^+ cells and the mean fluorescence intensity of the GFP signal was obtained from **A**. Gating was performed by excluding values where the intensity of GFP was below 10^3 (AU). The percentage of GFP^+ cells and the mean fluorescence intensity of events were obtained from gated events (n=1).

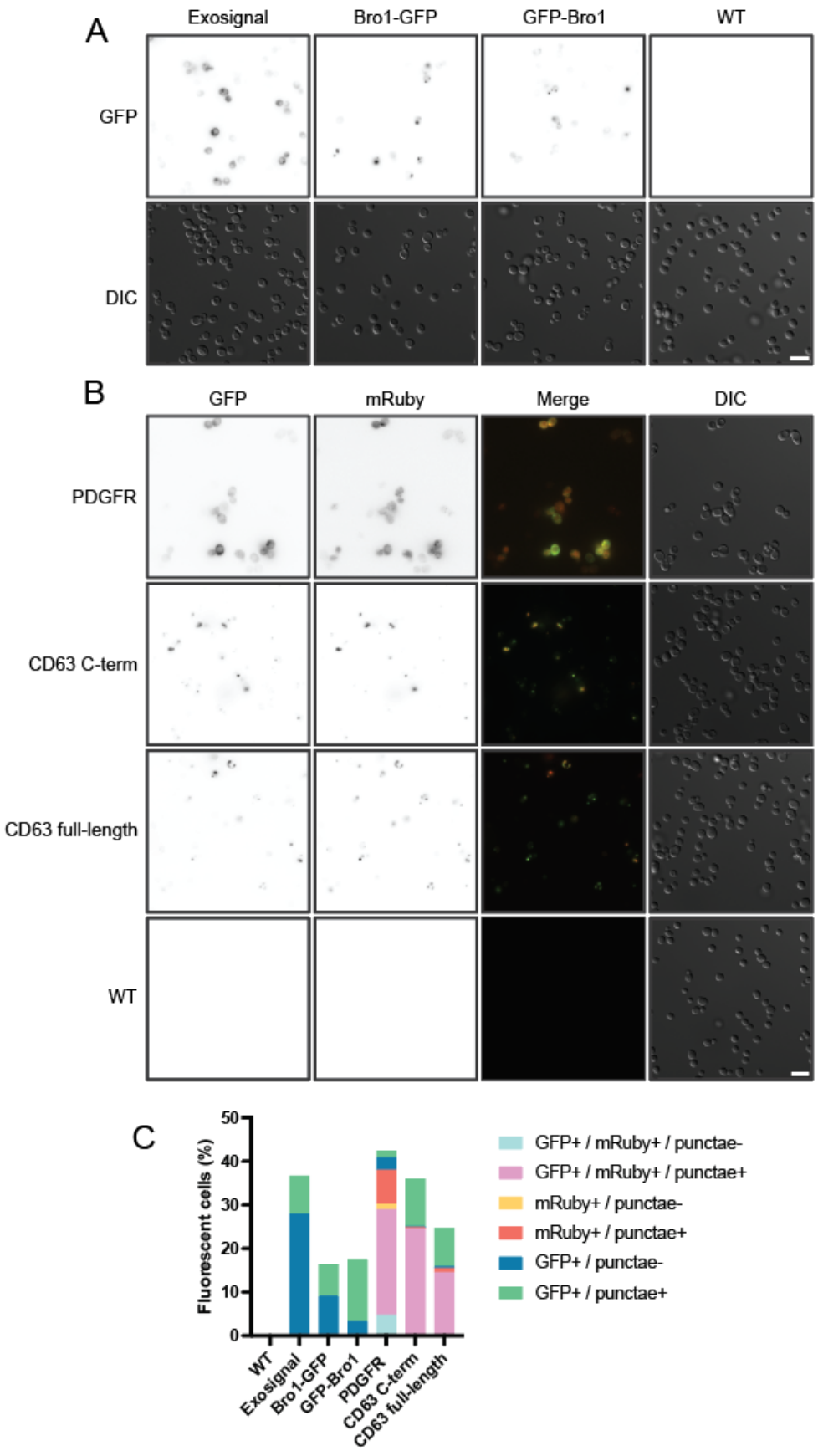
A
Exosignal
Bro1-GFP
GFP-Bro1
WT
GFP
DIC
B
GFP
mRuby
Merge
DIC
PDGFR
CD63 C-term
CD63 full-length
WT
C
Fluorescent cells (%)
50
40
30
20
10
0
WT
Exosignal
Bro1-GFP
GFP-Bro1
PDGFR
CD63 C-term
CD63 full-length
GFP+ / mRuby+ / punctae-
GFP+ / mRuby+ / punctae+
mRuby+ / punctae-
mRuby+ / punctae+
GFP+ / punctae-
GFP+ / punctae+

Figure 5. ExoTags are present at sites of exosome biogenesis

(A, B) Fluorescence micrographs of live cells expressing the panel of ExoTags fused to GFP or GFP and mRuby. Scale bar, 10 μm (n=3). **(C)** Proportion of fluorescent cells with respect to the presence of punctate structures. ≥ 100 cells were analyzed for each image. Live cells were counted using resulting micrographs and ImageJ software (Cell Counter plugin), and the percentage of fluorescent cells was calculated (n=3).

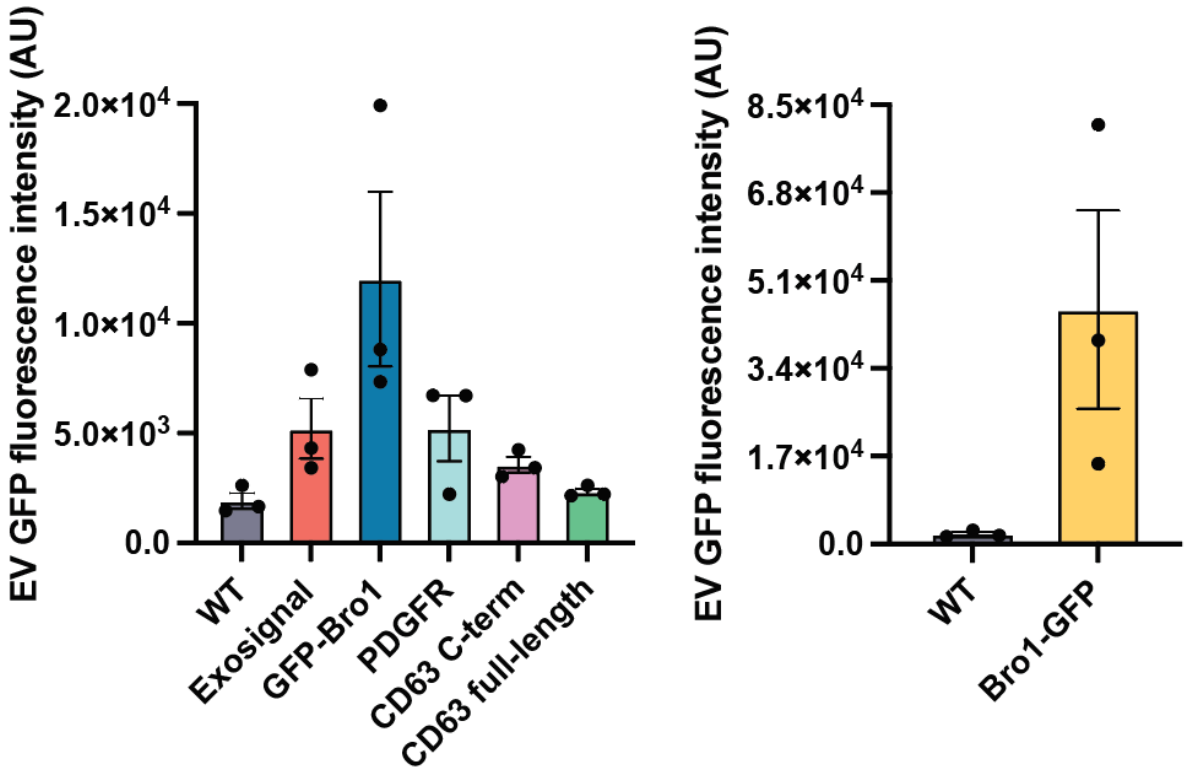

Figure 6. Genetically modified strains release engineered EVs

Florescence intensity of EV samples collected from WT, Exosignal, Bro1-GFP, GFP-Bro1, PDGFR, CD63 C-term and CD63 full-length strains. Both graphs are part of the same dataset. They have been separated to better demonstrate the fluorescence intensity of all EV samples. The data pertaining to EVs from WT cells are the same in both graphs. 100 µL of EV samples were measured for fluorometry assays using λex = 470 nm; λem = 510 nm (n=3). Mean ± S.E.M are shown.

3.2 EVs released from engineered cells retain their original structural characteristics

Successfully engineering EVs requires the implementation of bioactive elements (i.e. ExoTags and cargos) without the alteration of their size and round shape in order to minimize response variation during trials on recipient cells. The majority of EVs have been reported to possess a round shape and it has been established in the literature that exosomes are typically sized between 50 – 150 nm in diameter. Here, I attempted to confirm the presence of EVs isolated from engineered strains by visualizing their shape and measuring their size. Nanoparticle tracking analysis (NTA) is a standard method to estimate the size and concentration of EVs whereas transmission electron microscopy (TEM) is the most reliable approach to visualize their morphology. Analyzing EV isolates with these methods would provide some evidence regarding whether their shape and size have changed subsequent to the genetic modification of their hosts. Indeed, the particles isolated from the engineered strains show a similar distribution of size compared to EVs isolated from WT **(Figure 7A)**. Furthermore, images acquired via TEM demonstrated that EVs isolated from each strain possessed a round shape and were sized between 50 – 150 nm in diameter **(Figure 7B)**. It is worth mentioning that EV yields were greater for the Bro1-GFP, GFP-Bro1 and PDGFR strains **(Figure 7C)**. If the ExoTags were solely involved in cargo-loading, the cells should have released similar quantities of EVs. These results suggest that these tags additionally increase EV biogenesis, however, this puts into question my initial hypothesis of Bro1-GFP being the most efficient ExoTag across the panel as the increase in GFP fluorescence intensity **(Figure 6)** may be influenced by the greater quantity of exosomes present in isolates. These results prompt further investigation on a single-particle basis to further determine the efficiency of cargo-loading of each ExoTag.

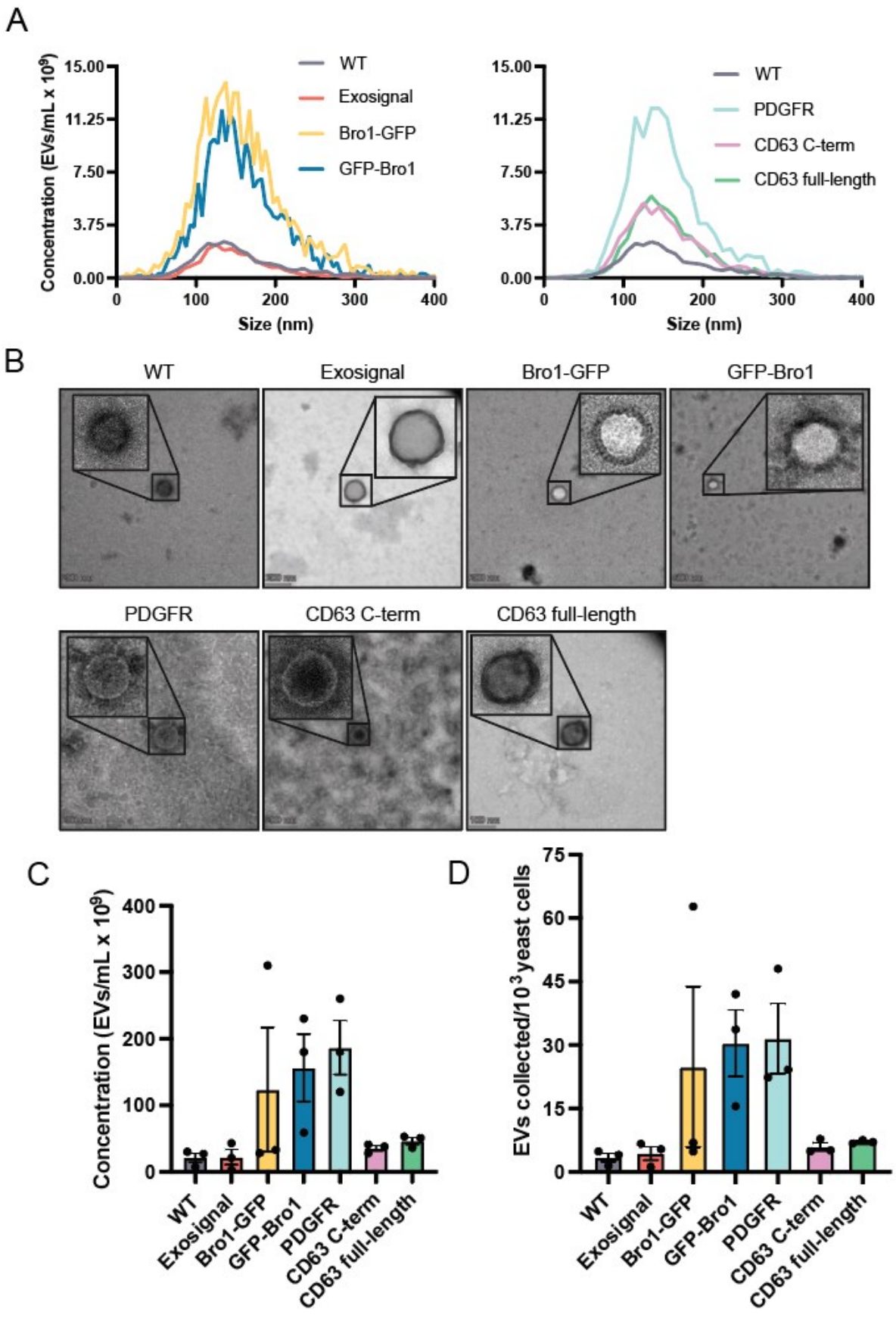
A
Concentration (EVs/mL x 10^9)
15.00
11.25
7.50
3.75
0.00
0
100
200
300
400
Size (nm)
WT
Exosignal
Bro1-GFP
GFP-Bro1
WT
PDGFR
CD63 C-term
CD63 full-length
B
WT
Exosignal
Bro1-GFP
GFP-Bro1
PDGFR
CD63 C-term
CD63 full-length
C
Concentration (EVs/mL x 10^9)
400
300
200
100
0
WT
Exosignal
Bro1-GFP
GFP-Bro1
PDGFR
CD63 C-term
CD63 full-length
D
EVs collected/10^3 yeast cells
75
60
45
30
15
0
WT
Exosignal
Bro1-GFP
GFP-Bro1
PDGFR
CD63 C-term
CD63 full-length

Figure 7. Cells release particles with characteristics of exosomes

(A) Distribution of particle concentrations based on size from NTA of EV samples collected from all strains (n=3). **(B)** Transmission electron micrographs of EVs samples. For better observation particles have been enhanced in the corner of images using Adobe Photoshop CC software (n=1). **(C)** Concentration of EVs isolated from all strains. Mean particle concentration values were provided by the Particle Metrix software (n=3). Mean ± S.E.M are shown. **(D)** Quantity of EVs released by yeast cells. The number of total EVs was obtained via multiplying the particle concentration by the final volume of isolated EVs. The number of cells was calculated by assuming an OD_{600} of 1 corresponded to 3 x 10^7 cells/mL as stated in BioNumbers database (BNID 100986, Milo et al., 2010) (n=3). Mean ± S.E.M are shown.

3.3 Exosignal is the most efficient ExoTag across the panel based on single particle analysis

I implemented nanoflow cytometry to detect the presence of GFP in individual particles which allowed me to examine the proportion of engineered EVs in each isolate. The most efficient ExoTag would be determined by finding the strain releasing the highest ratio of GFP^+ EVs with respect to native EVs as this would be a direct result of its capacity to localize to EVs. GFP was detected in EVs released by each genetically modified strain **(Figure 8A)**. The signal was detected to a much lower extent in WT, however, this could be due to background fluorescence. To find the ratio of GFP^+ EVs to native EVs, I multiplied the quantity of GFP^+ events by the dilution factor of the sample and divided this by the total amount of particles present in a read which was determined via NTA. On average, Exosignal is present in EVs at a higher proportion compared to other ExoTags tested in this panel **(Figure 8B).** To follow up on my results that initially suggested that Bro1-GFP was the most effective ExoTag **(Figure 6)**, I analyzed the quantity of GFP^+ EVs released with respect to the GFP^+ cells present in culture. This would further indicate whether any of the ExoTags used in this study influence exosome bioproduction by only considering the cells expressing EVClo plasmids. Indeed, despite releasing a lower proportion of GFP^+ EVs, the Bro1-GFP strain releases the highest quantity of engineered EVs for a given number of cells suggesting its involvement in exosome bioproduction. Furthermore, it is worth noting that PDGFR and CD63 C-term EVs exhibited higher GFP fluorescence intensity compared to other EVs, indicating that multiple ExoTags can be found on a single exosome **(Figure 8D)**. The enrichment of ExoTags on or in individual EVs may depend on how efficiently they are incorporated into the EV biogenesis pathway. This is a feature that would prove to be incredibly useful for the optimization of surface display and cargo-loading in EVs. Overall, the data obtained via nanoflow cytometry suggest that Exosignal is the most efficient candidate in terms of shuttling cargo to EVs. However, it is possible that a proportion of the events captured **(Figure 8A)** represent noise which may reduce GFP detection. This could put into question the reliability of this method to analyze EVs obtained from our pipeline, and therefore, definitive conclusions should not be drawn from these results. Alternatively, the fluorometry results suggest that Bro1 is the most efficient ExoTag across the panel (**Figure 6)**. This is expected as Bro1 is a yeast protein, which should be expressed with greater ease compared to the human ExoTags used in this study, and it is the ortholog to the

human EV marker ALIX, shown to be abundant in exosomes (Willms et al., 2016). These findings indicate yeast counterparts to human EV markers could be used as viable components for engineering EVs in *S. cerevisiae*.

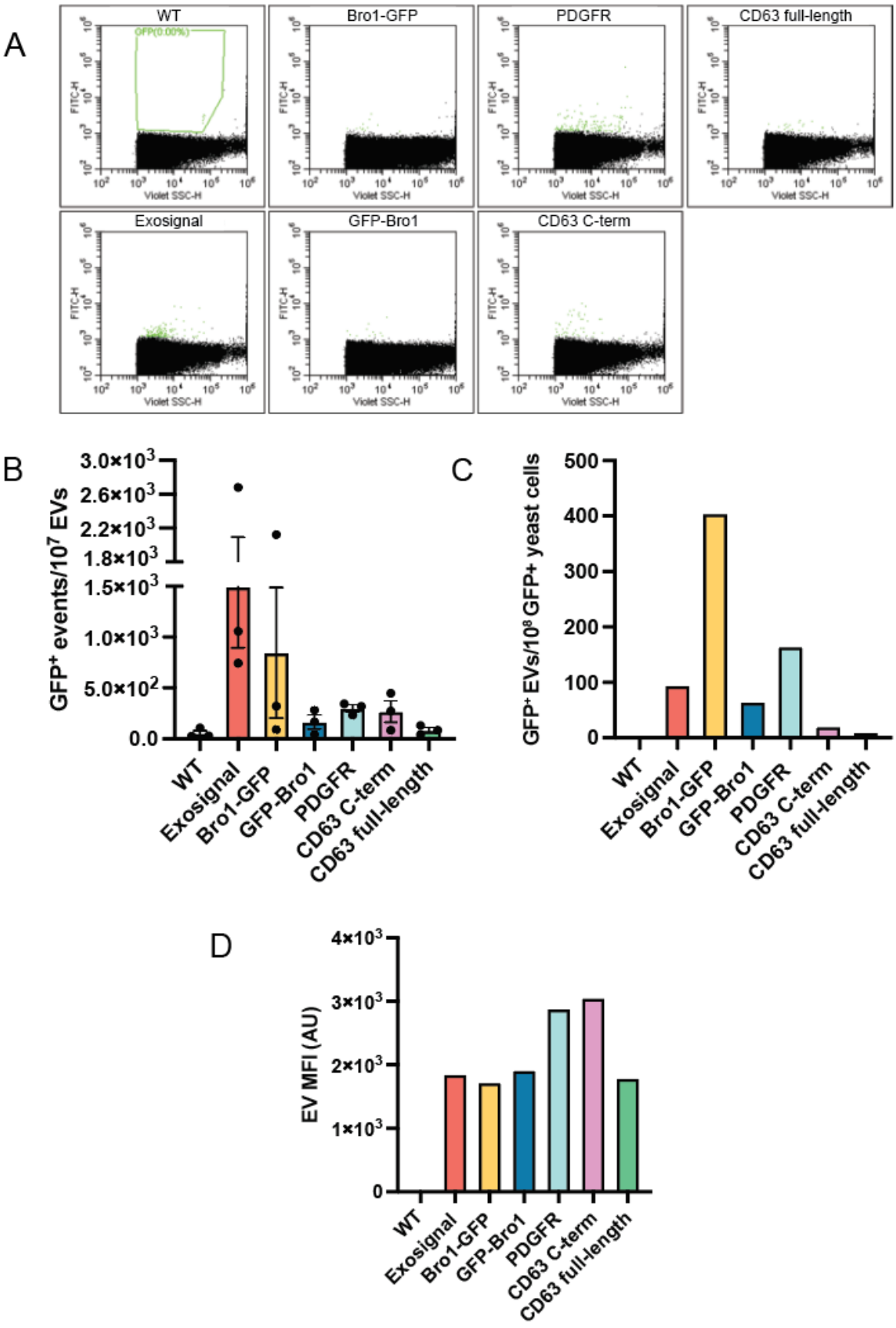
A
WT
Bro1-GFP
PDGFR
CD63 full-length
Exosignal
GFP-Bro1
CD63 C-term
FITC-H
Violet SSC-H
B
GFP+ events/10^7 EVs
3.0×10^3
2.6×10^3
2.2×10^3
1.8×10^3
1.5×10^3
1.0×10^3
5.0×10^2
0.0
C
GFP+ EVs/10^8 GFP+ yeast cells
500
400
300
200
100
0
WT
Exosignal
Bro1-GFP
GFP-Bro1
PDGFR
CD63 C-term
CD63 full-length
D
EV MFI (AU)
4×10^3
3×10^3
2×10^3
1×10^3
0

Figure 8. ExoTags possess varying EV localization capabilities

(A) Nanoflow cytometry analysis of EVs showing particle fluorescence intensity with respect side scattering. FITC-H corresponds to GFP intensity (AU). Prior to measurement, the sample was diluted to bring its concentration within the working range of the equipment (< 10,000 events/s) and 30 µL were measured (n=3). **(B)** The proportion of GFP^+ EVs released by genetically modified yeast cells. Values were obtained by multiplying the quantity of GFP^+ events measured in (A) by the dilution factor of the sample. These values were divided by the concentration of particles in each sample determined by NTA. Mean ± S.E.M are shown. **(C)** Quantity of GFP^+ EVs released by GFP^+ yeast cells (n=3). The total GFP^+ EVs yield was calculated by multiplying the proportion of GFP^+ EVs : GFP^- EVs by the total volume of isolated EV samples. The quantity of GFP^+ cells for each strain was calculated based on percentages of GFP^+ cells obtained via flow cytometry via nanoflow cytometry and NTA. The percentage of GFP^+ yeast cells was obtained via flow cytometry **(Figure 4B)**. Mean are shown. **(D)** Mean fluorescence intensity of GFP^+ EVs. The values obtained are based on gated events in (A) (shown in green). MFI was calculated using the Floreada software. Mean are shown.

CHAPTER 4 DISCUSSION

4.1 Laying the groundwork: demonstrating a toolkit for engineered EV bioproduction

To this day, most efforts to modify EVs have been performed using mammalian cell lines, which have provided an abundance of knowledge on EV biology and endogenous engineering strategies. However, the search for effective ExoTags is a slow and laborious process as the EV community has not addressed ways of systematically engineering strains for studying EV biology at scale. This can be due to the high costs associated with maintaining human cell lines and the limited molecular biology toolkits available for their genetic manipulation. In contrast, microbial systems demand fewer resources and allow for complex genetic engineering with unparalleled ease that are amenable for high-throughput workflows. This study is the first of its kind to combine methods from the mammalian EV engineering literature with sophisticated microbial genetic modification techniques to create a scalable platform for the bioproduction of designer EVs in *Saccharomyces cerevisiae*. The system termed "EVClo" is based on the highly characterized yeast toolkit (YTK) for modular, multipart assembly, allowing EV parts to easily fit into the YTK system as 3, 3a, 3b or 4a parts (Lee et al., 2015). EV cargos can enter the scheme as YTK parts or Gateway entry clones. This system could offer the ability to increase the output of engineered strains as it is a simple method for directional plasmid assembly, and yeast transformants can be easily obtained and screened. Furthermore, as there have been developments in tools to analyse individual nanosized particles, cargo loading and surface display capabilities of ExoTags can be reliably determined. If an EV marker is shown to efficiently localize to exosomes, further endogenous strategies to develop EV-based drugs in yeast can be performed by fusing therapeutic molecules to an ExoTag bound to a fluorescent reporter. This approach could be used to determine whether the presence of EV-bound cargo internalized by recipient cells results in therapeutic outcomes.

It is worth noting the drawback involved with this system with regards to comparing the efficiency of multiple ExoTags which stem from using a plasmid-based approach for strain generation. In this investigation, it was found that despite being housed in the same vector, ExoTag expression varied between strains. This interpretation can be drawn from the range in GFP^+ cells and their mean GFP fluorescence intensity **(Figure 4)**. These results may be

attributed to differences in plasmid copy numbers across cells which has been previously observed in yeast strains harboring plasmids with a 2 μm origin or replication (Dobson et al., 2005). Differences in cell-to-cell plasmid copy number may cause challenges in comparing the efficacy of multiple ExoTags as (in)decreased engineered EV yields could be a result from variations in construct expression than EV signals having altered localization capabilities. Nonetheless, developing a systematic approach for EV engineering will allow for the broad testing of ExoTags, which could accelerate our understanding of EV biology.

4.2 Future directions

Assessing the utility of a novel platform designed to streamline EV biology research must be performed at a small scale prior to pursuing larger studies that require significant amounts of time and resources. Here, I followed this principle by characterizing EVs from a panel of six strains expressing ExoTags and determined that Bro1 is the candidate that possesses the greatest cargo-loading capacity. However, in comparison with the mammalian literature, the total EV yields were incredibly low. For mammalian cells, depending on the isolation technique, culturing method and media and cell line, it is possible to obtain EV yields ranging from 2.0×10^4 to over 1.0×10^6 particles/cell (Kim et al., 2021; Grangier et al., 2021; Jackson and Marcus, 2023). This may raise the question regarding whether the platform described here would indeed be useful for EV bioproduction at an industrial scale. However, unlike the field of fungal EV biology, tremendous effort has been drawn into optimizing mammalian EV bioproduction, identifying EV-associated markers and developing systems to achieve higher cargo-loading efficiency. Considering that this is the first iteration of the engineered yeast EV bioproduction platform and that engineered fungal EV research is severely lacking, it is no surprise that the output of our system is suboptimal. Fortunately, there are strategies that could be implemented to improve our pipeline. These involve (1) adjusting the EV isolation protocol for this objective, (2) finding strains that promote greater EV release and (3) discovering more potent ExoTags suitable for a yeast platform.

In order to increase the yield of engineered EVs it may be worth further optimizing our protocol to identify the conditions that promote exosome release in yeast. It has been previously

demonstrated that different pools of EVs are released with respect to specific environmental conditions that cells are exposed to (Oliver, 2021). Additionally, multiple stressors can have an additive effect where multiple pools of EVs are released simultaneously. The exposure of both heat and osmotic stress to yeast cells results in a greater release of exosomes compared to subjecting cells to a single stressor (Oliver, 2021). Additionally, as yeast exosomes are believed to cross the cell wall via pores, it may be worthwhile to inflict cell wall damage to increase pore size. In a previous study, three industrial strains of *S. cerevisiae* were subjected to oxidative stress via the exposure of 10 mM diamide resulting in greater density and sizes of cell wall pores (de Souza Pereira and Geibel, 1999). This could increase EV release by damaging the barrier preventing the escape of exosomes. Furthermore, increasing the time yeast cells are subjected to heat shock may trigger a greater release of EVs. The protocol used in this study was developed to understand the role of yeast exosomes in conferring thermotolerance to heat stress and therefore may not be suitable for the purpose of maximizing engineered EV yields. In order to establish this system as a platform for EV bioproduction it may be useful to further optimize the yeast EV isolation protocol by testing the effects of multiple stressors (including those that damage the cell wall) and finetuning the time of EV release.

Creating a yeast strain which overexpresses one or many key components of the exosome biogenesis machinery could be a promising strategy for increasing EV yields. This would involve altering the exosome biogenesis pathway to promote their release. Studies have shown that deleting components of the ESCRT machinery resulted in reduced EV release in *C. albicans* (Zarnowski et al., 2018). Additionally, deletion mutants of Vps2, Vps23, Vps36 and Hse1 resulted in a decrease of yeast EV protein (Zhao et al., 2019). While this method of EV quantification may not represent the most precise measure of yield, it is still an indicative metric related to changes in EV release. By taking an opposite approach and overexpressing genes involved in EV biogenesis, it would be possible to bolster the cellular machinery responsible for the formation, packaging and release of exosomes. This strategy is supported by the results of this study and a colleague's previous work where the overexpression of Bro1, and TSG101 (the human ortholog of Vps23) resulted in the increase of EV release **(Figure 7)** (Logan, 2022). As the exosome biogenesis pathway has not been fully elucidated, altering the production of distinct ESCRT components may not always guarantee an increase in exosome production as their action

can be context specific in terms of environmental cues and the presence of different cargos. Nonetheless, this approach could pave the way for the development of yeast strains tailored for high-yield exosome production.

Finally, increasing the output of engineered EVs could be possible by incorporating more suitable ExoTags. Recent studies from the Brett lab have yielded valuable insights through proteomics analyses, identifying a set of yeast proteins that are abundant in isolated EVs (Oliver, 2021). Some of these include enzymes involved in metabolism and cell wall remodelling, as well as heat shock proteins. Harnessing proteins that have been found to be abundant in yeast EVs could significantly increase the efficiency of engineered EV production which holds the potential to overcome the limitations encountered with human ExoTags. Furthermore, determining whether candidate proteins shuttle cargo to the surface or the lumen of EVs could be achieved by incorporating a luciferase reporter in the system. This was demonstrated by Zheng and colleagues who used ThermoLuc to study the lumenal and surface loading capacities of EV-associated proteins (2023). Leveraging the endogenous protein landscape of yeast-derived EVs, novel strategies can be explored for optimizing this pipeline, offering a new direction for advancing the engineered exosome bioproduction platform.

While this attempt to engineer yeast strains for endogenous loading of biological cargos into exosomes using human ExoTags has faced challenges, it reveals critical avenues for future exploration. The results of this study underscore the intricate regulatory networks governing EV cargo incorporation and emphasize the necessity for a nuanced understanding of the interactions between human EV markers with the yeast exosome biogenesis machinery. Nonetheless, the platform retains considerable promise and ongoing research offers multiple avenues for improvement. One key focus involves optimizing the extracellular vesicle isolation protocol to enhance the EV release. Additionally, the exploration of yeast strains with a potentially increased capacity for EV biogenesis remains a hopeful strategy. Lastly, another avenue involves the selection of more promising ExoTags suitable for effective cargo loading.

Developing an efficient method to produce engineered exosomes using yeast as a bioproduction platform has significant implications in clinical settings. As they represent a

promising drug delivery vehicle, they could facilitate the transport of therapeutic cargo directly to specific cells or tissues and enhance the efficacy of therapeutic agents while minimizing off-target effects and reducing systemic toxicity. Furthermore, the scalable and cost-effective nature of a yeast-based production platform could pave the way for large-scale manufacturing of engineered EVs which is necessary for translating laboratory findings into clinically viable applications. The development of standardized methods for EV production in yeast could streamline manufacturing processes, making engineered EVs more readily available for clinical use. Overall, the efficient production of engineered EVs using yeast as a bioproduction platform holds the potential to significantly advance personalized medicine and drug delivery, contributing to the development of innovative and more targeted therapeutic interventions.

REFERENCES

Aaronson, S., Behrens, U., Orner, R., and Haines, T.H. 1971. Ultrastructure of intracellular and extracellular vesicles, membranes, and myelin figures produced by Ochromonas danica. *J Ultrastruct Res*. 35(5):418–430. doi:10.1016/s0022-5320(71)80003-5.

Andreou, A.I., and Nakayama, N. 2018. Mobius Assembly: A versatile Golden-Gate framework towards universal DNA assembly. *PLoS One*. 13(1):e0189892. doi:10.1371/journal.pone.0189892.

Andreu, Z., and Yáñez-Mó, M. 2014. Tetraspanins in extracellular vesicle formation and function. *Front. Immunol*. 5:442. doi: 10.3389/fimmu.2014.00442

Antes, T. J., Middleton, R. C., Luther, K. M., Ijichi, T., Peck, K. A., Liu, W. J., Valle, J., Echavez, A. K., and Marbán, E. Targeting extracellular vesicles to injured tissue using membrane cloaking and surface display. *J Nanobiotechnol* 16, 61 (2018). https://doi.org/10.1186/s12951-018-0388-4

Bao, H., Bi, C., Li, W., Zhang, X., Zhang, H., Meng, B., and Fu, K. 2017. Chimeric Antigen Receptor-Engineered Exosome As a Drug Delivery System in Mantle Cell Lymphoma. *Blood*. 130(Supplement 1):5561. doi:10.1182/blood.V130.Suppl_1.5561.5561.

Bean, B.D.M., Whiteway, M., and Martin, V.J.J. 2022. The MyLO CRISPR-Cas9 toolkit: a markerless yeast localization and overexpression CRISPR-Cas9 toolkit. *G3 (Bethesda)*. 12(8):jkac154. doi:10.1093/g3journal/jkac154.

Bertrand, N., and Leroux, J. C. 2012. The journey of a drug-carrier in the body: an anatomo-physiological perspective. *J Control Release*. 161(2):152–163. doi:10.1016/j.jconrel.2011.09.098.

Buzas, E.I. 2023. The roles of extracellular vesicles in the immune system. *Nat Rev Immunol*. 23(4):236–250. doi:10.1038/s41577-022-00763-8.

Cao, M., Isaac, R., Yan, W., Ruan, X., Jiang, L., Wan, Y., Wang, J., Wang, E., Caron, C., Neben, S., Drygin, D., Pizzo, D. P., Wu, X., Liu, X., Chin, A. R., Fong, M. Y., Gao, Z., Guo, K., Fadare, O., Schwab, R. B., … Wang, S. E. 2022. Cancer-cell-secreted extracellular vesicles suppress insulin secretion through miR-122 to impair systemic glucose homeostasis and contribute to tumour growth. *Nat Cell Biol*. 24(6):954–967. doi:10.1038/s41556-022-00919-7.

Chargaff, E., and West, R. 1946. The biological significance of the thromboplastic protein of blood. *J Biol Chem*. 166(1):189–197.

Chigaleĭchik, A.G., Belova, L.A., Grishchenko, V.M., and Rylkin, S.S. Nekotorye svoĭstva ékstratselliuliarnykh vezikul drozhzheĭ Candida tropicalis vyrashchennykh na n-aklanakh [Several properties of the extracellular vesicles of Candida tropicalis yeasts grown on n-alkanes]. *Mikrobiologiia*. 1977;46(3):467-471.

Costa-Silva, B., Aiello, N. M., Ocean, A. J., Singh, S., Zhang, H., Thakur, B. K., Becker, A., Hoshino, A., Mark, M. T., Molina, H., Xiang, J., Zhang, T., Theilen, T. M., García-Santos, G., Williams, C., Ararso, Y., Huang, Y., Rodrigues, G., Shen, T. L., Labori, K. J., … Lyden, D. 2015. Pancreatic cancer exosomes initiate pre-metastatic niche formation in the liver. *Nat Cell Biol*. 17(6):816–826. doi:10.1038/ncb3169.

Couch, Y., Buzàs, E. I., Di Vizio, D., Gho, Y. S., Harrison, P., Hill, A. F., Lötvall, J., Raposo, G., Stahl, P. D., Théry, C., Witwer, K. W., and Carter, D. R. F. 2021. A brief history of nearly EV-erything - The rise and rise of extracellular vesicles. *J Extracell Vesicles*. 10(14):e12144. doi: 10.1002/jev2.12144.

Dang, X. T. T., Kavishka, J. M., Zhang, D. X., Pirisinu, M., and Le, M. T. N. 2020. Extracellular Vesicles as an Efficient and Versatile System for Drug Delivery. *Cells*. 9(10):2191. doi:10.3390/cells9102191.

Delcayre, A., Estelles, A., Sperinde, J., Roulon, T., Paz, P., Aguilar, B., Villanueva, J., Khine, S., and Le Pecq, J. B. 2005. Exosome Display technology: applications to the development of new diagnostics and therapeutics. *Blood Cells Mol Dis*. 35(2):158-68. doi: 10.1016/j.bcmd.2005.07.003.

Denby, L., Work, L. M., Seggern, D. J., Wu, E., McVey, J. H., Nicklin, S. A., and Baker, A. H. 2007. Development of renal-targeted vectors through combined in vivo phage display and capsid engineering of adenoviral fibers from serotype 19p. *Mol Ther*. 15(9):1647-54. doi: 10.1038/sj.mt.6300214.

Dixson, A. C., Dawson, T. R., Di Vizio, D., and Weaver, A. M. 2023. Context-specific regulation of extracellular vesicle biogenesis and cargo selection. *Nat Rev Mol Cell Biol*.:1–23. doi:10.1038/s41580-023-00576-0.

Dobson, M. J., Pickett, A. J., Velmurugan, S., Pinder, J. B., Barrett, L. A., Jayaram, M., & Chew, J. S. 2005. The 2μm Plasmid Causes Cell Death in Saccharomyces cerevisiae with a Mutation in Ulp1 Protease. *Mol Cell Biol*. 25(10):4299–4310. doi:10.1128/MCB.25.10.4299-4310.2005.

Ferreira, J. V., da Rosa Soares, A., Ramalho, J., Máximo Carvalho, C., Cardoso, M. H., Pintado, P., Carvalho, A. S., Beck, H. C., Matthiesen, R., Zuzarte, M., Girão, H., van Niel, G., and Pereira, P. 2022. LAMP2A regulates the loading of proteins into exosomes. *Sci Adv*. 8(12):eabm1140. doi:10.1126/sciadv.abm1140.

French, K. C., Antonyak, M. A., and Cerione, R. A. 2017. Extracellular vesicle docking at the cellular port: Extracellular vesicle binding and uptake. *Semin Cell Dev Biol*. 67:48-55. doi:10.1016/j.semcdb.2017.01.002

Fuhrmann, G., Serio, A., Mazo, M., Nair, R., and Stevens, M. M. 2015. Active loading into extracellular vesicles significantly improves the cellular uptake and photodynamic effect of porphyrins. *J Control Release*. 205:35–44. doi:10.1016/j.jconrel.2014.11.029.

Gelperina, S., Kisich, K., Iseman, M. D., and Heifets, L. 2005. The potential advantages of nanoparticle drug delivery systems in chemotherapy of tuberculosis. *Am J Respir Crit Care Med*. 172(12):1487–1490. doi:10.1164/rccm.200504-613PP.

Ghosh, D., and Barry, M. A. 2005. Selection of muscle-binding peptides from context-specific peptide-presenting phage libraries for adenoviral vector targeting. *J Virol*. 79(21):13667-72. doi: 10.1128/JVI.79.21.13667-13672.2005.

Gong, X. H., Liu, H., Wang, S. J., Liang, S. W., and Wang, G. G. 2019. Exosomes derived from SDF1-overexpressing mesenchymal stem cells inhibit ischemic myocardial cell apoptosis and promote cardiac endothelial microvascular regeneration in mice with myocardial infarction. *J Cell Physiol*. 234(8):13878–13893. doi:10.1002/jcp.28070.

Gowen, A., Shahjin, F., Chand, S., Odegaard, K. E., and Yelamanchili, S. V. 2020. Mesenchymal Stem Cell-Derived Extracellular Vesicles: Challenges in Clinical Applications. *Front Cell Dev Biol*. 8:149. doi:10.3389/fcell.2020.00149

Grangier, A., Branchu, J., Volatron, J., Piffoux, M., Gazeau, F., Wilhelm, C., and Silva, A. K. A. 2021. Technological advances towards extracellular vesicles mass production. *Adv Drug Deliv Rev*. 176:113843. doi:10.1016/j.addr.2021.113843.

Guo, S., Perets, N., Betzer, O., Ben-Shaul, S., Sheinin, A., Michaelevski, I., Popovtzer, R., Offen, D., and Levenberg, S. 2019. Intranasal Delivery of Mesenchymal Stem Cell Derived Exosomes Loaded with Phosphatase and Tensin Homolog siRNA Repairs Complete Spinal Cord Injury. *ACS Nano*. 13(9):10015–10028. doi:10.1021/acsnano.9b01892.

Haney, M. J., Klyachko, N. L., Zhao, Y., Gupta, R., Plotnikova, E. G., He, Z., Patel, T., Piroyan, A., Sokolsky, M., Kabanov, A. V., and Batrakova, E. V. 2015. Exosomes as drug delivery vehicles for Parkinson's disease therapy. *J Control Release*. 207:18–30. doi:10.1016/j.jconrel.2015.03.033.

Harrell, C. R., Jovicic, N., Djonov, V., Arsenijevic, N., and Volarevic, V. 2019. Mesenchymal Stem Cell-Derived Exosomes and Other Extracellular Vesicles as New Remedies in the Therapy of Inflammatory Diseases. *Cells*. 8(12):1605. doi:10.3390/cells8121605.

Hartmann, A., Muth, C., Dabrowski, O., Krasemann, S., and Glatzel, M. 2017. Exosomes and the Prion Protein: More than One Truth. *Front. Neurosci*. 11:194. doi: 10.3389/fnins.2017.00194

Henne, W.M., Buchkovich, N.J., and Emr, S.D. 2011. The ESCRT pathway. *Dev Cell*. 21(1):77–91. doi:10.1016/j.devcel.2011.05.015.

Hoshino, A., Kim, H. S., Bojmar, L., Gyan, K. E., Cioffi, M., Hernandez, J., Zambirinis, C. P., Rodrigues, G., Molina, H., Heissel, S., Mark, M. T., Steiner, L., Benito-Martin, A., Lucotti, S., Di Giannatale, A., Offer, K., Nakajima, M., Williams, C., Nogués, L., Pelissier Vatter, F. A., … Lyden, D. 2020. Extracellular Vesicle and Particle Biomarkers Define Multiple Human Cancers. *Cell*. 182(4):1044-1061.e18. doi:10.1016/j.cell.2020.07.009.

Jackson, K.K., and Marcus, R.K. 2023. Rapid isolation and quantification of extracellular vesicles from suspension-adapted human embryonic kidney cells using capillary-channeled polymer fiber spin-down tips. *Electrophoresis*. 44(1–2):190–202. doi:10.1002/elps.202200149.

Jayasinghe, M. K., Tan, M., Peng, B., Yang, Y., Sethi, G., Pirisinu, M., and Le, M. T. N. 2021. New approaches in extracellular vesicle engineering for improving the efficacy of anti-cancer therapies. *Semin Cancer Biol*. 74:62–78. doi:10.1016/j.semcancer.2021.02.010.

Johnson, R. C., Zhu, D., Augustin-Voss, H. G., and Pauli, B. U. 1993. Lung endothelial dipeptidyl peptidase IV is an adhesion molecule for lung-metastatic rat breast and prostate carcinoma cells. *J Cell Biol*. 121(6):1423–1432. doi:10.1083/jcb.121.6.1423.

Johnstone, R. M., Adam, M., Hammond, J. R., Orr, L., and Turbide, C. 1987. Vesicle formation during reticulocyte maturation. Association of plasma membrane activities with released vesicles (exosomes). *J Biol Chem*. 262(19):9412–9420.

Johnstone, R.M., Mathew, A., Mason, A.B., and Teng, K. 1991. Exosome formation during maturation of mammalian and avian reticulocytes: evidence that exosome release is a major route for externalization of obsolete membrane proteins. *J Cell Physiol*. 147(1):27–36. doi:10.1002/jcp.1041470105.

Kachroo, A. H., Laurent, J. M., Akhmetov, A., Szilagyi-Jones, M., McWhite, C. D., Zhao, A., and Marcotte, E. M. 2017. Systematic bacterialization of yeast genes identifies a near-universally swappable pathway. Barkai N, editor. *eLife*. 6:e25093. doi:10.7554/eLife.25093.

Kachroo, A. H., Laurent, J. M., Yellman, C. M., Meyer, A. G., Wilke, C. O., and Marcotte, E. M. 2015. Evolution. Systematic humanization of yeast genes reveals conserved functions and genetic modularity. *Science*. 348(6237):921–925. doi:10.1126/science.aaa0769.

Kamerkar, S., LeBleu, V. S., Sugimoto, H., Yang, S., Ruivo, C. F., Melo, S. A., Lee, J. J., and Kalluri, R. 2017. Exosomes facilitate therapeutic targeting of oncogenic KRAS in pancreatic cancer. *Nature*. 546(7659):498–503. doi:10.1038/nature22341.

Kim, J. Y., Rhim, W. K., Seo, H. J., Lee, J. Y., Park, C. G., and Han, D. K. 2021. Comparative Analysis of MSC-Derived Exosomes Depending on Cell Culture Media for Regenerative Bioactivity. *Tissue Eng Regen Med*. 18(3):355–367. doi:10.1007/s13770-021-00352-1.

Kooijmans, S. A. A., Stremersch, S., Braeckmans, K., de Smedt, S. C., Hendrix, A., Wood, M. J. A., Schiffelers, R. M., Raemdonck, K., and Vader, P. 2013. Electroporation-induced siRNA precipitation obscures the efficiency of siRNA loading into extracellular vesicles. *J Control Release*. 172(1):229–238. doi:10.1016/j.jconrel.2013.08.014.

Krylova, S.V., and Feng, D. 2023. The Machinery of Exosomes: Biogenesis, Release, and Uptake. *Int J Mol Sci*. 24(2):1337. doi:10.3390/ijms24021337.

Lamesch, P., Li, N., Milstein, S., Fan, C., Hao, T., Szabo, G., Hu, Z., Venkatesan, K., Bethel, G., Martin, P., Rogers, J., Lawlor, S., McLaren, S., Dricot, A., Borick, H., Cusick, M. E., Vandenhaute, J., Dunham, I., Hill, D. E., and Vidal, M. 2007. hORFeome v3.1: a resource of human open reading frames representing over 10,000 human genes. *Genomics*. 89(3):307-15. doi: 10.1016/j.ygeno.2006.11.012.

Lee, M. E., DeLoache, W. C., Cervantes, B., and Dueber, J. E. 2015. A Highly Characterized Yeast Toolkit for Modular, Multipart Assembly. *ACS Synth Biol*. 4(9):975–986. doi:10.1021/sb500366v.

Lee, R., Ko, H. J., Kim, K., Sohn, Y., Min, S. Y., Kim, J. A., Na, D., and Yeon, J. H. 2019. Anti-melanogenic effects of extracellular vesicles derived from plant leaves and stems in mouse melanoma cells and human healthy skin. *J Extracell Vesicles*. 9(1):1703480. doi:10.1080/20013078.2019.1703480.

Li, J., Zhang, Q., Pang, Z., Wang, Y., Liu, Q., Guo, L., and Jiang, X. 2012. Identification of peptide sequences that target to the brain using in vivo phage display. *Amino Acids*. 42(6):2373–2381. doi:10.1007/s00726-011-0979-y.

Liu, X., Li, X., Zhu, W., Zhang, Y., Hong, Y., Liang, X., Fan, B., Zhao, H., He, H., and Zhang, F. 2020. Exosomes from mesenchymal stem cells overexpressing MIF enhance myocardial repair. *J Cell Physiol*. 235(11):8010–8022. doi:10.1002/jcp.29456.

Logan, C.J. 2022. Humanization of Yeast Exosome Protein Selection Machinery to Investigate Functional Evolutionary Conservation. MSc (Biology) Thesis. Concordia University. Montreal, QC, Canada.

Milo, R., Jorgensen, P., Moran, U., Weber, G., and Springer, M. 2010. BioNumbers--the database of key numbers in molecular and cell biology. *Nucleic Acids Res*. 38(Database issue):D750-753. doi:10.1093/nar/gkp889.

Mulcahy, L. A., Pink, R. C., and Carter, D. R. 2014. Routes and mechanisms of extracellular vesicle uptake. *J Extracell Vesicles*. 3. doi:10.3402/jev.v3.24641.

van Niel, G., Carter, D. R. F., Clayton, A., Lambert, D. W., Raposo, G., and Vader, P. 2022. Challenges and directions in studying cell–cell communication by extracellular vesicles. *Nat Rev Mol Cell Biol*. 23(5):369–382. doi:10.1038/s41580-022-00460-3.

Ohno, S., Takanashi, M., Sudo, K., Ueda, S., Ishikawa, A., Matsuyama, N., Fujita, K., Mizutani, T., Ohgi, T., Ochiya, T., Gotoh, N., and Kuroda, M. 2013. Systemically injected exosomes targeted to EGFR deliver antitumor microRNA to breast cancer cells. *Mol Ther*. 21(1):185-91. doi: 10.1038/mt.2012.180.

Oliveira, D. L., Nakayasu, E. S., Joffe, L. S., Guimarães, A. J., Sobreira, T. J., Nosanchuk, J. D., Cordero, R. J., Frases, S., Casadevall, A., Almeida, I. C., Nimrichter, L., and Rodrigues, M. L. 2010. Characterization of yeast extracellular vesicles: evidence for the participation of different pathways of cellular traffic in vesicle biogenesis. *PLoS One*. 5(6):e11113. doi: 10.1371/journal.pone.0011113.

Oliver, J. 2021. Saccharomyces cerevisiae communities share extracellular vesicles for protection from heat stress. MSc (Biology) Thesis. Concordia University. Montreal, QC, Canada.

Pirisinu, M. 2023. The Long Journey of Extracellular Vesicles towards Global Scientific Acclamation. *Adv Pharm Bull*. 13(3):489–501. doi:10.34172/apb.2023.049.

Pulliero, A., Pergoli, L., LA Maestra, S., Micale, R. T., Camoirano, A., Bollati, V., Izzotti, A., and DE Flora, S. 2019. Extracellular vesicles in biological fluids. A biomarker of exposure to cigarette smoke and treatment with chemopreventive drugs. *J Prev Med Hyg*. 60(4):E327-E336. doi: 10.15167/2421-4248/jpmh2019.60.4.1284.

Raposo, G., Nijman, H. W., Stoorvogel, W., Liejendekker, R., Harding, C. V., Melief, C. J., and Geuze, H. J. 1996. B lymphocytes secrete antigen-presenting vesicles. *J Exp Med*. 183(3):1161–1172. doi:10.1084/jem.183.3.1161.

Ratajczak, J., Miekus, K., Kucia, M., Zhang, J., Reca, R., Dvorak, P., and Ratajczak, M. Z. 2006. Embryonic stem cell-derived microvesicles reprogram hematopoietic progenitors: evidence for horizontal transfer of mRNA and protein delivery. *Leukemia*. 20(5):847–856. doi:10.1038/sj.leu.2404132.

Reece-Hoyes, J. S., and Walhout, A. J. M. 2018. Gateway Recombinational Cloning. *Cold Spring Harb Protoc*. 2018(1):pdb.top094912. doi: 10.1101/pdb.top094912.

Research and Markets. 2023. Exosomes Market Size, Share & Trends Analysis Report By Product (Kits & Reagents, Services), By Application (Cancer, CVD), By Workflow (Isolation Methods, Downstream Analysis), By End-use, And Segment Forecasts, 2023 - 2030. [accessed 2023 Sep 29]. https://www.researchandmarkets.com/reports/4479695/exosomes-market-size-share-and-trends-analysis.

Saksena, S., Sun, J., Chu, T., and Emr, S. D. 2007. ESCRTing proteins in the endocytic pathway. *Trends Biochem Sci*. 32(12):561–573. doi:10.1016/j.tibs.2007.09.010.

Shi, X., Cheng, Q., Hou, T., Han, M., Smbatyan, G., Lang, J. E., Epstein, A. L., Lenz, H. J., and Zhang, Y. 2020. Genetically Engineered Cell-Derived Nanoparticles for Targeted Breast Cancer Immunotherapy. *Mol Ther*. 28(2):536–547. doi:10.1016/j.ymthe.2019.11.020.

Skogberg, G., Lundberg, V., Berglund, M., Gudmundsdottir, J., Telemo, E., Lindgren, S., and Ekwall, O. 2015. Human thymic epithelial primary cells produce exosomes carrying tissue-restricted antigens. Immunol Cell Biol. 93(8):727–734. doi:10.1038/icb.2015.33.

Skokos D, Botros HG, Demeure C, Morin J, Peronet R, Birkenmeier G, Boudaly S, Mécheri S. 2003. Mast cell-derived exosomes induce phenotypic and functional maturation of dendritic cells and elicit specific immune responses in vivo. *J Immunol*. 170(6):3037–3045. doi:10.4049/jimmunol.170.6.3037.

Song, Y., Kim, Y., Ha, S., Sheller-Miller, S., Yoo, J., Choi, C., and Park, C. H. 2021. The emerging role of exosomes as novel therapeutics: Biology, technologies, clinical applications, and the next. *Am J Reprod Immunol*. 85(2):e13329. doi: 10.1111/aji.13329.

de Souza Pereira, R., and Geibel, J. 1999. Direct observation of oxidative stress on the cell wall of Saccharomyces cerevisiae strains with atomic force microscopy. *Mol Cell Biochem*. 201(1):17–24. doi:10.1023/A:1007007704657.

Staufer, O., Dietrich, F., Rimal, R., Schröter, M., Fabritz, S., Boehm, H., Singh, S., Möller, M., Platzman, I., and Spatz, J. P. 2021. Bottom-up assembly of biomedical relevant fully synthetic extracellular vesicles. *Sci Adv*. 7(36):eabg6666. doi:10.1126/sciadv.abg6666.

Stickney, Z., Losacco, J., McDevitt, S., Zhang, Z., and Lu, B. 2016. Development of exosome surface display technology in living human cells. *Biochem Biophys Res Commun*. 472(1):53–59. doi:10.1016/j.bbrc.2016.02.058.

Stoicheva, N. G., and Hui, S. W. 1994. Electrofusion of cell-size liposomes. *Biochim Biophys Acta*. 1195(1):31-8. doi: 10.1016/0005-2736(94)90005-1.

Sun, D., Zhuang, X., Xiang, X., Liu, Y., Zhang, S., Liu, C., Barnes, S., Grizzle, W., Miller, D., and Zhang, H. G. 2010. A Novel Nanoparticle Drug Delivery System: The Anti-

inflammatory Activity of Curcumin Is Enhanced When Encapsulated in Exosomes. *Mol Ther*. 18(9):1606–1614. doi:10.1038/mt.2010.105.

Teng, F., and Fussenegger, M. 2021. Shedding Light on Extracellular Vesicle Biogenesis and Bioengineering. *Adv Sci*. 8(1):2003505. doi:10.1002/advs.202003505.

Théry, C., Duban, L., Segura, E., Véron, P., Lantz, O., and Amigorena, S. 2002. Indirect activation of naïve CD4+ T cells by dendritic cell–derived exosomes. *Nat Immunol*. 3(12):1156–1162. doi:10.1038/ni854.

Thodey, K., Galanie, S., and Smolke, C.D. 2014. A microbial biomanufacturing platform for natural and semisynthetic opioids. *Nat Chem Biol*. 10(10):837–844. doi:10.1038/nchembio.1613.

Usman, W. M., Pham, T. C., Kwok, Y. Y., Vu, L. T., Ma, V., Peng, B., Chan, Y. S., Wei, L., Chin, S. M., Azad, A., He, A. B., Leung, A. Y. H., Yang, M., Shyh-Chang, N., Cho, W. C., Shi, J., and Le, M. T. N. 2018. Efficient RNA drug delivery using red blood cell extracellular vesicles. *Nat Commun*. 9(1):2359. doi:10.1038/s41467-018-04791-8.

Utsugi-Kobukai, S., Fujimaki, H., Hotta, C., Nakazawa, M., and Minami, M. 2003. MHC class I-mediated exogenous antigen presentation by exosomes secreted from immature and mature bone marrow derived dendritic cells. *Immunol Lett*. 89(2):125–131. doi:10.1016/S0165-2478(03)00128-7.

Wang, J. H., Forterre, A. V., Zhao, J., Frimannsson, D. O., Delcayre, A., Antes, T. J., Efron, B., Jeffrey, S. S., Pegram, M. D., and Matin, A. C. 2018. Anti-HER2 scFv-Directed Extracellular Vesicle-Mediated mRNA-Based Gene Delivery Inhibits Growth of HER2-Positive Human Breast Tumor Xenografts by Prodrug Activation. *Mol Cancer Ther*. 17(5):1133–1142. doi:10.1158/1535-7163.MCT-17-0827.

Wang, X., Zhang, H., Yang, H., Bai, M., Ning, T., Li, S., Li, J., Deng, T., Ying, G., and Ba, Y. 2018. Cell-derived Exosomes as Promising Carriers for Drug Delivery and Targeted Therapy. *Curr Cancer Drug Targets*. 18(4):347–354.

Wang, Z., Popowski, K. D., Zhu, D., de Juan Abad, B. L., Wang, X., Liu, M., Lutz, H., De Naeyer, N., DeMarco, C. T., Denny, T. N., Dinh, P. C., Li, Z., and Cheng, K. 2022. Exosomes decorated with a recombinant SARS-CoV-2 receptor-binding domain as an inhalable COVID-19 vaccine. *Nat Biomed Eng*. 6(7):791–805. doi:10.1038/s41551-022-00902-5.

Wei, Z., Qiao, S., Zhao, J., Liu, Y., Li, Q., Wei, Z., Dai, Q., Kang, L., and Xu, B. 2019. miRNA-181a over-expression in mesenchymal stem cell-derived exosomes influenced inflammatory response after myocardial ischemia-reperfusion injury. *Life Sci*. 232:116632. doi:10.1016/j.lfs.2019.116632.

Wiest, E.F., and Zubair, A.C. 2020. Challenges of manufacturing mesenchymal stromal cell–derived extracellular vesicles in regenerative medicine. *Cytotherapy*. 22(11):606–612. doi:10.1016/j.jcyt.2020.04.040.

Wiklander, O. P., Nordin, J. Z., O'Loughlin, A., Gustafsson, Y., Corso, G., Mäger, I., Vader, P., Lee, Y., Sork, H., Seow, Y., Heldring, N., Alvarez-Erviti, L., Smith, C. I., Le Blanc, K., Macchiarini, P., Jungebluth, P., Wood, M. J., and Andaloussi, S. E. 2015. Extracellular vesicle in vivo biodistribution is determined by cell source, route of administration and targeting. *J Extracell Vesicles*. 4:26316. doi: 10.3402/jev.v4.26316.

Williams, R.L., and Urbé, S. 2007. The emerging shape of the ESCRT machinery. *Nat Rev Mol Cell Biol*. 8(5):355–368. doi:10.1038/nrm2162.

Willms, E., Johansson, H. J., Mäger, I., Lee, Y., Blomberg, K. E., Sadik, M., Alaarg, A., Smith, C. I., Lehtiö, J., El Andaloussi, S., Wood, M. J., and Vader, P. 2016. Cells release subpopulations of exosomes with distinct molecular and biological properties. *Sci Rep*. 6(1):22519. doi: 10.1038/srep22519.

Wolfers, J., Lozier, A., Raposo, G., Regnault, A., Théry, C., Masurier, C., Flament, C., Pouzieux, S., Faure, F., Tursz, T., Angevin, E., Amigorena, S., and Zitvogel, L. 2001. Tumor-derived exosomes are a source of shared tumor rejection antigens for CTL cross-priming. *Nat Med.* 7(3):297-303. doi: 10.1038/85438.

Yang, Z., Shi, J., Xie, J., Wang, Y., Sun, J., Liu, T., Zhao, Y., Zhao, X., Wang, X., Ma, Y., Malkoc, V., Chiang, C., Deng, W., Chen, Y., Fu, Y., Kwak, K. J., Fan, Y., Kang, C., Yin, C., Rhee, J., … Lee, L. J. 2020. Large-scale generation of functional mRNA-encapsulating exosomes via cellular nanoporation. *Nat Biomed Eng*. 4(1):69-83. doi: 10.1038/s41551-019-0485-1.

Zahler, S., Ghazi, N.G., and Singh, A.D. 2019. Principles and Complications of Chemotherapy. In: Singh, A., Damato, B. (eds) *Clinical Ophthalmic Oncology*. Springer, Cham. https://doi.org/10.1007/978-3-030-04489-3_13

Zarnowski, R., Sanchez, H., Covelli, A. S., Dominguez, E., Jaromin, A., Bernhardt, J., Mitchell, K. F., Heiss, C., Azadi, P., Mitchell, A., and Andes, D. R. 2018. Candida albicans biofilm-induced vesicles confer drug resistance through matrix biogenesis. *PLoS Biol*. 16(10):e2006872. doi: 10.1371/journal.pbio.2006872.

Zhang, B., Wang, M., Gong, A., Zhang, X., Wu, X., Zhu, Y., Shi, H., Wu, L., Zhu, W., Qian, H., and Xu, W. 2015. HucMSC-Exosome Mediated-Wnt4 Signaling Is Required for Cutaneous Wound Healing. *Stem Cells*. 33(7):2158-68. doi: 10.1002/stem.1771.

Zhao, K., Bleackley, M., Chisanga, D., Gangoda, L., Fonseka, P., Liem, M., Kalra, H., Al Saffar, H., Keerthikumar, S., Ang, C.S., Adda, C.G., Jiang, L., Yap, K., Poon, I.K., Lock, P., Bulone, V., Anderson, M., and Mathivanan, S. 2019 Extracellular vesicles secreted by Saccharomyces cerevisiae are involved in cell wall remodelling. *Commun Biol*. 2:305. doi: 10.1038/s42003-019-0538-8.

Zheng, W., Rädler, J., Sork, H., Niu, Z., Roudi, S., Bost, J. P., Görgens, A., Zhao, Y., Mamand, D. R., Liang, X., Wiklander, O. P. B., Lehto, T., Gupta, D., Nordin, J. Z., & El Andaloussi, S. 2023. Identification of scaffold proteins for improved endogenous engineering of extracellular vesicles. *Nat Commun*. 14(1):4734. doi: 10.1038/s41467-023-40453-0.

Zimmermann, A., Kainz K., Andryushkova, A., Hofer, S., Madeo, F., and Carmona-Gutierrez, D. 2016. Autophagy: one more Nobel Prize for yeast. *Microb Cell*. 3(12):579–581. doi:10.15698/mic2016.12.544.